



Mesozoic and Cenozoic evolution of the Central European lithosphere



T. Meier^{a,*}, R.A. Soomro^{a,1}, L. Viereck^b, S. Lebedev^c, J.H. Behrmann^d, C. Weidle^a, L. Cristiano^a, R. Hanemann^b

^a Christian-Albrechts University Kiel, Institute for Geosciences, Otto-Hahn-Platz 1, 24118 Kiel, Germany

^b Friedrich-Schiller University Jena, Institute for Geosciences, Burgweg 11, 07749 Jena, Germany

^c Dublin Institute for Advanced Studies, Geophysics Section, 5 Merrion Square, Dublin 2, Ireland

^d GEOMAR, Helmholtz-Zentrum für Ozeanforschung Kiel, Dynamics of the ocean floor, Wischhofstrasse 1-3, 24148 Kiel, Germany

ARTICLE INFO

Article history:

Received 30 January 2016

Received in revised form 21 July 2016

Accepted 12 September 2016

Available online 13 September 2016

Keywords:

Seismic tomography

Continental lithosphere

Lithosphere-asthenosphere boundary

Intraplate volcanism

Central Europe

ABSTRACT

The upper crust of central Europe preserves a mosaic of tectonic blocks brought together by the Caledonian and Variscan Orogenies. The lower crust, in contrast, appears to have undergone extensive reworking: the flat Moho across broad areas and the absence of contrasts in seismic properties across tectonic boundaries suggest that the Moho and lower crust are, effectively, younger than the upper crust. The evolution of the mantle lithosphere below the Moho has been particularly difficult to constrain. In this paper, we use seismic, geological and geochemical evidence to show that central Europe's mantle lithosphere has evolved continuously throughout the Mesozoic and Cenozoic Eras, with episodes of lithospheric thinning causing surface uplift and volcanism and lithospheric thickening – subsidence and sedimentation. High-resolution surface wave tomography reveals a strong spatial correlation between locations of recent basaltic volcanism and currently thin lithosphere. We infer that intraplate volcanism further back in the geological past is also an indication of lithospheric thinning at the time. The north-central Europe's lithosphere was, thus, thinned at the time of the Permian volcanism, with its subsequent, Post-Permian cooling and thickening causing the subsidence and sedimentation in the North German and neighboring basins. This explains the presence of Permian volcanics atop presently thickened lithosphere. South of these basins, lithospheric thinning (evidenced by seismic data) is associated with the volcanism of the Central European Cenozoic Igneous Province and surface uplift. Thin lithosphere here also correlates spatially with high melting rates, high silica contents, high temperatures and shallow magma generation. This synthesis highlights the dynamic nature of the lithosphere-asthenosphere boundary beneath central Europe and, more generally, Phanerozoic continents. The boundary's depth varies in time; its deepening (lithospheric cooling and thickening) causes subsidence and sedimentation; its shallowing (lithospheric thinning by thermal erosion or delamination) is marked with uplift and intraplate volcanism.

© 2016 Published by Elsevier B.V.

1. Introduction

Central and western Europe is one of the parts of the world where modern geology developed as a science and, after centuries of scrutiny, the geological record across the region is very well documented. Plate tectonics has brought modern explanations for the formation of the European landmass in the Caledonian and Variscan Orogenies in the Paleozoic Era, and for active tectonics of the Africa-Eurasia convergence. Yet, a key piece of the puzzle is still missing. Whereas abundant evidence is available on the structure and evolution of the upper and middle crust, much less is known of the evolution of the deeper part of the plate, including the lower crust and, in particular, the mantle lithosphere. The deep evolution of the lithosphere and its interactions with the underlying asthenosphere are linked to the uplift and subsidence

of the Earth's surface and to intraplate volcanism across central Europe. The difficulty in obtaining conclusive observational evidence, however, has meant that both the deep lithospheric evolution and its effect on surface tectonics and volcanism remain uncertain.

The lithosphere is the mechanically strong, outer layer of the Earth that makes up the tectonic plates. It comprises the crust and the uppermost, coldest part of the mantle – the lithospheric mantle. The lithosphere coincides, roughly, with the Earth's upper thermal boundary layer, in which temperature is relatively low and increases with depth along steep conductive geotherms. The conductive geotherms reach the mantle adiabat near the bottom of the lithosphere. Further down, heat transfer is primarily by convection within the warm, mechanically weak sublithospheric mantle (the asthenosphere).

The thermal evolution of the lithosphere looks fairly simple beneath the oceans: it cools and thickens monotonically from its birth at mid-ocean ridges to its ultimate subduction into the deep mantle at subduction zones, as seen clearly in recent tomographic models (e.g., Schaeffer and Lebedev, 2013). This dominant pattern is broken only by hotspots,

* Corresponding author.

E-mail address: meier@geophysik.uni-kiel.de (T. Meier).

¹ Now Seismic Studies Programme, Nilore, Islamabad 4000, Pakistan.

which re-heat the oceanic lithosphere as it passes over them. After passing a hotspot, however, the plate would normally resume the cooling and thickening process.

There is continuing debate on whether the thickness of the oceanic lithosphere reaches a maximum at around 80 m.y. of the lithospheric age (the “plate model”) or whether, instead, plate thickening according to the “half-space cooling model” (e.g., Davis and Lister, 1974; McKenzie et al., 2005) continues until the age of the oldest oceans on Earth today. The apparent lack of heat-flow dependence on the lithospheric age for old oceans (>80 Myr) and the flattening of the old oceans’ bathymetry are evidence for the plate model (e.g., Stein and Stein, 1992, 2015). Yet, depth profiles of shear velocity and azimuthal anisotropy beneath the oceans appear to evolve with the seafloor age following the half-space cooling model, according to recent tomographic models (e.g., Becker et al., 2014; Schaeffer et al., 2016). In any case, it is clear that the oceanic lithosphere, hotspots aside, cools and thickens at least until 80 Myr of age, and then it either remains equally cold and thick or may continue to cool and thicken further.

Compared to oceanic lithosphere, continental lithosphere is characterized by much greater complexity in its structure and evolution, owing, in part, to its much greater range of ages. The oldest ocean floor within today’s major ocean basins is Jurassic (around 180 Ma in the western Pacific), and the oldest preserved in-situ oceanic crust may be a remnant of the Neotethys Ocean beneath the Ionian Sea and the east Mediterranean basin, still only Triassic in age (230–270 Ma) (Müller et al., 2008). In contrast, the oldest intact fragments of continental crust are >4 billion years old (Bowring and Williams, 1999), and it is the Archean cratons (>2.5 Ga in age) that form the cores of today’s continents. The global igneous record shows pronounced continental crust age peaks at 2.7 and 1.9 Ga, with some compilations suggesting another peak at 1.2 Ga (e.g., Condie, 1998; Hawkesworth et al., 2010). This record may not represent the true rates of crustal generation due to preservation artefacts (e.g. Gurnis and Davies, 1986) but it is clear that the evolution of the continental lithosphere measures >3 billions of years.

A natural consequence of the cooling of the lithosphere at the Earth’s surface is that it will grow in thickness, up to a point when its bottom portion becomes unstable and sinks into the underlying mantle (Bird, 1979). Mantle lithosphere beneath Archean cratons is compositionally buoyant due to its depletion in basaltic components (e.g., Jordan, 1975, 1988). For this reason, the lithosphere beneath cratons can cool and grow to a greater thickness than elsewhere (although it can be partly rejuvenated and eroded: Foley, 2008; Legendre et al., 2012). In global and continent-scale seismic tomography models, cratons stand out as the most prominent high-velocity anomalies down to 200–250 km depths, which reflects their coldest and thickest lithosphere (Debayle and Ricard, 2012; French et al., 2013; Schaeffer and Lebedev, 2015).

Phanerozoic continental lithosphere, in contrast, never reaches thicknesses comparable to that of the cratons. Density of the Phanerozoic subcontinental lithospheric mantle (SCLM in the following) is higher than that of the Archean SCLM (at the same pressure and temperature), limiting the maximum Phanerozoic lithospheric thickness to about 150 km (Poudjom Djomani et al., 2001).

Like oceanic lithospheric mantle, the SCLM can also be thermally eroded; it then cools and thickens again. These processes lead to and are manifested by tectonic and magmatic consequences at the Earth’s surface. Thermal erosion and thinning of the SCLM are accompanied by uplift and magmatism, whereas cooling of the lithosphere causes subsidence and development of basins (e.g., Poudjom Djomani et al., 2001). Stretching of the lithosphere can cause passive upwelling of the asthenospheric mantle, also followed by subsidence due to cooling (McKenzie, 1978). The thickening of the SCLM, however, is limited by delamination (Bird, 1979). Phanerozoic SCLM shows pronounced lateral variations, even when relatively stable, that is, not in immediate proximity to active orogens (e.g. Cloetingh et al., 2007; Legendre et al., 2012). This is a manifestation of dynamic processes involving the SCLM, the lithosphere–asthenosphere boundary (LAB), and the

asthenosphere. Although these processes are likely to have major effects on continental tectonics and intraplate volcanism, they are still poorly understood.

Phanerozoic central Europe is a very suitable location to study these processes. Its lithosphere has been amalgamated by a series of Phanerozoic continent–continent collisions of Gondwana-derived terranes during the Caledonian and Variscan orogenies (e.g. Franke and Oncken, 1990; Berthelsen, 1992; Pharaoh, 1999; Thybo et al., 2002; Franke, 2006). The subsequent episodes of intraplate volcanism and sedimentary–basin development (e.g. Ziegler, 1990; Scheck and Bayer, 1999; van Wees et al., 2000; Ziegler and Dèzes, 2006; Lustrino and Wilson, 2007; Torsvik et al., 2008) are indications for the rejuvenation and cooling of the SCLM, respectively (as we discuss in detail in the following). The seismic properties of the crust in central Europe have been studied extensively (e.g. EUGENO-S working group, 1988; Meissner and Bortfeld, 1990; BABEL Working Group, 1993; Rabbel et al., 1995; MONA LISA Working Group, 1997; Grad et al., 2005). R. Meissner – to whom this special volume is dedicated – initiated and was involved in a number of deep seismic soundings of the crust in central Europe. The major findings of these initiatives are that (1) the crust is relatively thin (<35 km), most of it with a rather uniform thickness of 28 km to 32 km, (2) average crustal seismic velocities are rather low, (3) no expressions of terrane boundaries can be found in the lower crust, and (4) there is widespread reflectivity in the lower crust (Meissner et al., 1991; Meissner and Tanner, 1993; Meissner, 1999; Meissner et al., 2006; Artemieva and Meissner, 2012). From these observations, Meissner and co-workers inferred that the recent location of the crust–mantle boundary (Moho) in the area is younger than the tectonic age of the brittle upper crust, implying that the lower crust has been deformed during or after the Variscan orogeny.

In the northern part of the Variscan orogenic belt, basins formed in the Lower Permian (Rotliegend), with differential tectonic movements in the crust coming to a standstill in the Middle Permian (e.g. van Wees et al., 2000). The central European lithosphere has been further affected by the Permian volcanic event with a peak activity at about 290 Ma (Torsvik et al., 2008). There is evidence for widespread volcanic activity, especially in the Permian basins south of the East European Craton (EEC, Ziegler, 1990). It was followed by Mesozoic basin development in central Europe and the southern North Sea (e.g. Ziegler, 1990), with wide areas of epicontinental platform sedimentation. Van Wees et al. (2000) concluded that cooling of the lithosphere after thermal erosion in the Permian played a major role for the basin development. The sedimentation record is punctuated in many places, and comprises alternations of shallow water clastics, platform and basin carbonates, and occurrences of evaporites, mainly in the Middle and Upper Triassic. The Mesozoic sediments are unconformably superposed on Lower Permian (Rotliegend) clastics forming post-orogenic molasse-type deposits of considerable thickness in confined basins, and/or Upper Permian (Zechstein) evaporites and associated mudstones. In the Cenozoic, large areas in the south of central Europe were above sea level, but in Northern Germany and the North Sea subsidence produced basins with sedimentary fills more than three kilometers thick, mainly fine to coarse clastics. Further south and west, basin formation and subsidence in the Cenozoic are intricately connected to the European Cenozoic Rift System (e.g. Dèzes et al., 2004), which is made up of the Limagne, Bresse, Upper Rhine, Lower Rhine and Eger Graben structures, to name the most important ones.

There are only a few locations of Mesozoic volcanism south of the EEC and in central Europe, the volcanic field of Delitzsch-Bitterfeld and of the Northern Upper Rhine Graben (Odenwald, Sprendlinger Horst) (Schmitt et al., 2007; Krüger et al., 2013). But there is widespread Cenozoic volcanism in central Europe. Numerous intraplate volcanic fields stretch broadly parallel to the Alpine front between the Eifel (Germany) and Silesia (Poland) and form the northern E–W oriented zone of the Central European Cenozoic Igneous Province (CECIP, Wimmenauer, 1974; Wedepohl and Baumann, 1999; Lustrino and Wilson, 2007). As

listed in Table 1 and indicated in Fig. 1 they comprise the volcanic fields of the Hocheifel (No. 2 in Table 1, Huckenholz and Büchel, 1988; Jung et al., 2006), West and East Eifel (Nos. 1 & 3, Schmincke, 2007), Siebengebirge (No. 4, Jung et al., 2012; Kolb et al., 2012; Schubert et al., 2015), Westerwald (No. 5, Haase et al., 2004), Vogelsberg (No. 6, Jung and Masberg, 1998; Bogaard and Wörner, 2003), Hessian Depression (No. 7, Wedepohl, 1985), Rhön (No. 8, Jung and Hoernes, 2000; Meyer et al., 2002; Jung et al., 2005), Heldburg Dyke Swarm (No. 9, Huckenholz and Werner, 1990), Upper Palatinate (No. 10, Huckenholz and Schröder, 1985), Ohre Rift (Nos. 11, 12, 13, Ulrych et al., 1999, 2008, 2011), Lusatia (No. 14, Büchner et al., 2015), Lower Silesia (No. 15, Blusztain and Hart, 1989; Ladenberger et al., 2004; Badura et al., 2005), and Bruntal, eastern Moravia (No. 16, Cajz et al., 2012). Some smaller volcanic fields are located separately in SW Germany: Kaiserstuhl (No. 17), Hegau (No. 18) and Urach (No. 19, Brey and Keller, 1982; Geyer and Gwinner, 1984; Hegner et al., 1995; Wimmenauer, 2003; Schreiner, 2008).

In this paper, we present high resolution surface wave tomography of the lithosphere and asthenosphere in central Europe and relate the results to the location and composition of Cenozoic intraplate volcanic fields. We put together geophysical and geological evidence on the structure and Post-Permian evolution of the lithosphere and suggest a model for the Mesozoic and Cenozoic evolution of the post-orogenic SCLM in central Europe.

2. Brief overview of seismic studies of the European lithosphere

High-resolution seismic images can help to improve our understanding of the SCLM and its relationship to surface tectonics and volcanism. The central European lithosphere has been investigated extensively over decades of seismic reflection and refraction profiling, particularly in the 1980s and 1990s. In addition to resolving the architecture of the European crust, the controlled-source profiles have also clearly shown that sub-Moho reflectivity is in general low, concordant with global observations of Phanerozoic extensional zones (DEKORP, Meissner and Rabbel, 1999). Exceptions to the rule in central Europe (north of the Alps) are mantle reflections dipping from the Moho into the mantle north of the Harz Mountains, upper mantle reflections

associated with the Caledonian collision of Baltica with East Avalonia in the North Sea (BIRPS, Klempner and Matthews, 1987 and MONA LISA, Abramovitz and Thybo, 2000) and in the southern Baltic Sea (BABEL Working Group, 1991). The latter feature has been interpreted as a seismic image of a Precambrian subduction zone.

Overall, the Moho in central Europe is relatively flat, even across crustal terrane boundaries. Average crustal velocities are found to be relatively low, and sub-Moho seismic velocities are largely homogeneous, with only few localized deviations (Kraichgau, Hessian depression, Aichroth et al., 1992). These observations have prompted the interpretation that the Pre-Variscan lower crust and mantle lithosphere did not survive the Variscan orogeny and that they have been delaminated (Meissner and Rabbel, 1999; Artemieva and Meissner, 2012).

The SCLM itself is most commonly investigated by passive seismic methods, including seismic tomography and receiver functions. Seismic tomography yields either 3D models of the subsurface (usually, the distributions of P- or S-wave velocities within the crust and mantle) or 2D maps of the phase or group velocities of surface waves. The tomographic models are smoothed, due to approximations in the wave propagation, limited data coverage, the applied parametrization, and smoothness constraints. Receiver functions, in contrast, are used for the detection of sharp crustal and upper mantle discontinuities beneath seismic stations.

First seismic tomographic studies of central Europe date back to the 1980s, after permanent networks have been installed across the continent in the 1970s. In northern Europe, Calcagnile (1982) derived the first map of the lithospheric thickness of the Baltic Shield from surface wave measurements, estimating the thickness at >170 km (as compared to the 200–250-km estimates of today). The Baltic Shield's lithosphere has now been imaged, with varying resolution, by numerous surface wave studies and waveform inversions on the global scale (Trampert and Woodhouse, 1995; Masters et al., 2000; Zhou et al., 2006; Peter et al., 2008; Lebedev and van der Hilst, 2008; Boschi et al., 2009; Ritsema et al., 2011; Khan et al., 2011) and regional scales (Ritzwoller and Levshin, 1998; Villaseñor et al., 2001; Bruneton et al., 2004; Levshin et al., 2007; Weidle and Maupin, 2008; Legendre et al., 2012; Rickers et al., 2013), and also in body wave tomography on global (e.g. Grand et al., 1997; Grand, 2002) and regional (Spakman, 1990) scales. Seismic velocity anomalies are strongly positive in the mantle

Table 1
Location and main geochemical properties of volcanic fields within the CECIP plotted in Figs. 8 and 9. With the age of activity as indicated if $^{40}\text{Ar}/^{39}\text{Ar}$ (Ar) or K/Ar (K) ages are available. Data are taken from: Hoch-Eifel – Jung et al., 2006; Fekiacova et al., 2007a, 2007b; West- and East-Eifel – Mertes and Schmincke, 1985; Schmincke, 2007; Siebengebirge – Kolb et al., 2012; Jung et al., 2012; Westerwald – Lippolt and Todt, 1978; Haase et al., 2004; Vogelsberg – Bogaard and Wörner, 2003; Lower Hessian – Wedepohl, 1985; Rhön – Jung and Hoernes, 2000; Abratis et al., 2007; Heldburg Dyke Swarm – own data, Huckenholz and Werner, 1990; Upper Palatinate – Rohrmüller et al., 2005; Huckenholz and Schröder, 1985; Vogtland – Abratis et al., 2009; Doupovské Hory, České Středohoří – Ulrych et al., 1999, 2011; Haase and Renno, 2008; Labe (Elbe) Zone – Vaněčková et al., 1993; Ulrych et al., 2008; Lusatia – Büchner et al., 2015; Lower Silesia – Badura et al., 2005; Bruntal, eastern Moravia – Cajz et al., 2012; Kaiserstuhl, Hegau – Keller, 2008; Urach – Hegner et al., 1995.

Volcanic field	No. in Fig. 8	End of main activity in Ma	Average degree and range of partial melting in %	Average SiO ₂ content of primary magmas in %	Min. temperature in °C (Green and Falloon, 1998)	Depth in km (Green, 1972)
West Eifel	1	<0.1 (Ar)	2–5	42	1260	90
Hocheifel	2	35 (Ar)	3–6	43	1270	80
East Eifel	3	<0.1 (Ar)	5–8	44	1280	70
Siebengebirge	4	6 (Ar)	5–9	45	1295	60
Westerwald	5	20 (K)	5–8	44	1280	70
Vogelsberg AB/OT	6	16–19 (Ar)	8–13	50	1340	40
Vogelsberg BAS		14–19 (Ar)	4–6	45	1295	
Hessian Depression	7	13 (K)	5–10	47	1310	60
Rhön	8	18 (Ar)	5–7	44	1280	70
Heldburg Dyke Swarm	9	12 (Ar)	(4–7)	43	1270	70
Upper Palatinate	10	19 (Ar)	(3–6)	42	1260	80
Vogtland Mariánské Lázně Fault Zone	11	20 (K)	(2–3)	38	1200	110
		<1 (K)				
Ohre Rift	12	15 (K)	(4–7)	43	1270	70
Labe Zone	13	22 (K)	(2–3)	38	1200	110
Lusatia	14	22 (Ar)	(3–6)	42	1260	90
Lower Silesia	15	21 (K)	(4–7)	44	1280	70
Bruntal, eastern Moravia	16	0.8–4 (K)	(4–6)	43	1270	80
Kaiserstuhl	17	16 (A)	(5–8)	44	1280	70
Hegau	18	11 (K)	(3–4)	39	1230	100
Urach	19	11 (K)	(2–3)	38	1200	110

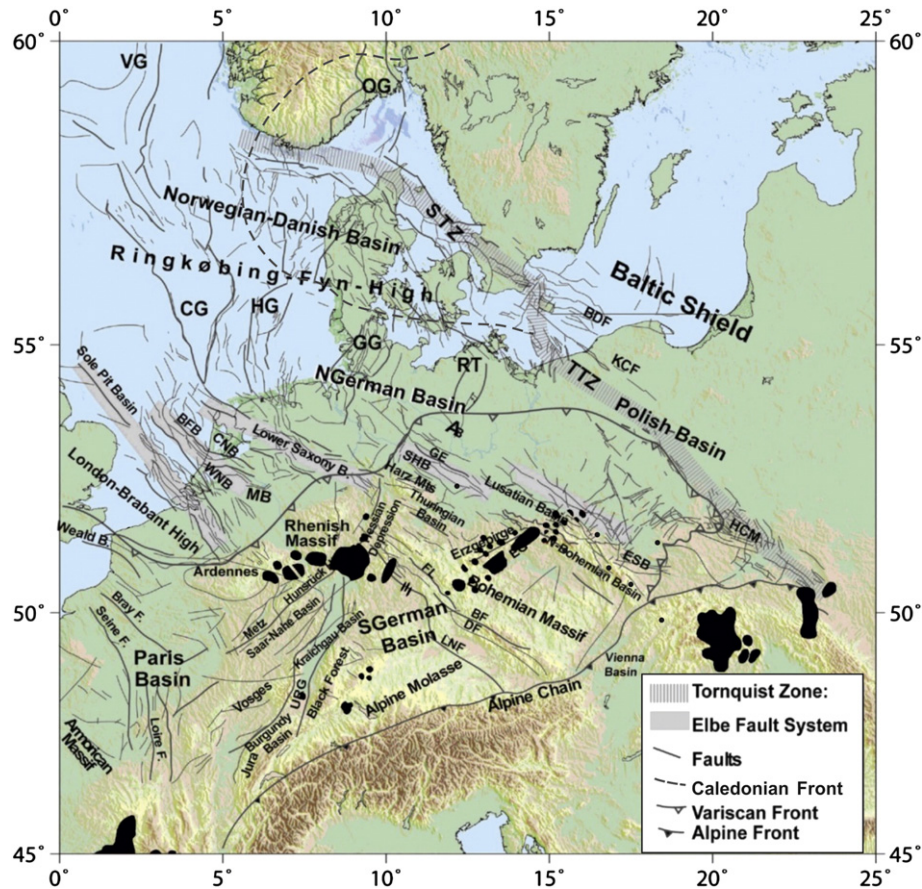


Fig. 1. Tertiary and Quaternary volcanic fields in Central Europe (dark black areas). VG: Viking Graben, OG: Oslo Graben, STZ: Sorgenfrei-Tornquist Zone, CG: Central Graben, HG: Horn Graben, GG: Glückstadt Graben, RT: Rheinsberg Trough, TTZ: Tornquist-Teisseyre Zone, BDF: Bornholm-Darłowo Fault Zone, KCF: Koszalin-Chojnice Fault Zone, MB: Brabant Massif, WNB: West Netherlands Basin, BFB: Broad Fourteens Basin, CNB: Central Netherlands Basin, SHB: Subhercynian Basin, GE: Gardelegen Escarpment, AB: Altmark Basin, ESB: Holy Cross Mountains, FL: Frankonian Lineament, DF: Donau Fault, BF: Bavarian Fault, LNF: Landshut-Neuoetting Fault, URG: Upper Rhine Graben. After Wilson and Downes (1991), van Balen et al. (2000), McCann (2008), Scheck-Wenderoth et al. (2008).

lithosphere down to about 150 km decreasing gradually further down, to bottom of the mantle lithosphere. Furthermore, tomographic studies indicate lateral heterogeneity within the mantle lithosphere of this craton, likely related to metasomatism (e.g. Bruneton et al., 2004; Legendre et al., 2012; Pedersen et al., 2013) as well as thermal erosion at the margins of the craton (e.g. Legendre et al., 2012; Maupin et al., 2013).

Receiver function observations across the craton has been interpreted as evidence for smaller depths of the lithospheric base at 160–200 km, with indications for horizontal layering within the mantle lithosphere, possibly related to the assembly of the shield (e.g. Olsson et al., 2007; Kind et al., 2013).

Across the Trans-European Suture Zone (TESZ) the transition to Phanerozoic Europe is generally associated with a distinct step in lithospheric thickness from ~200 km on the East European Platform to ~100 km in central Europe, a feature visible in all tomographic models (Zielhuis and Nolet, 1994; Nolet and Zielhuis, 1994; Schweitzer, 1995; Alsina and Snieder, 1996; Marquering and Snieder, 1996; Villaseñor et al., 2001; Cotte and Pedersen, 2002; Plomerova et al., 2002; Gregersen et al., 2010; Legendre et al., 2012; Schaeffer and Lebedev, 2013) as well as Receiver Function studies (Geissler et al., 2010; Kind et al., 2013; Knapmeyer-Endrun et al., 2013) although the sharp transition observed around the Tornquist-Teisseyre Zone (TTZ) in the southeast becomes more gradual towards the Sorgenfrei-Tornquist Zone (STZ) in the northwest (Gregersen et al., 2010; Soomro et al., 2016).

In central Europe, lateral variations in seismic velocities in the mantle lithosphere are overall rather small but there are substantial variations in the lithospheric thickness. The LAB across Europe is found to undulate around central depths of about 100 km (Babuška et al., 1984; Babuška

and Plomerová, 1992; Geissler et al., 2010; Knapmeyer-Endrun et al., 2013; Maystrenko and Scheck-Wenderoth, 2013) except for the region of the Rhenish Massif (Ritter et al., 2001; Budweg et al., 2006; Mathar et al., 2006; Seiberlich et al., 2013) and the Pannonian Basin (Dando et al., 2011; Legendre et al., 2012) where the lithosphere is significantly thinner. Variations in lithospheric thickness from temperature models are similar (>200 km on EEP, ~150 km in western Europe, ~50 km in the Eifel, Goes et al., 2000; Scheck-Wenderoth and Maystrenko, 2013). Modelling of heat flow observations for mantle geotherms is difficult due to the heterogeneity in crustal structure as well as recent tectonic activity in many areas but existing models confirm a thermal thickness of 100–150 km over most parts of Variscan Europe (Artemieva et al., 2006; Scheck-Wenderoth and Maystrenko, 2013).

The sub-lithospheric upper mantle beneath central Europe is generally characterized by low S-wave velocities from about 100 to 300 km depth (Zielhuis and Nolet, 1994; Marquering and Snieder, 1996; Bijwaard and Spakman, 2000; Villaseñor et al., 2001). These observations are largely persistent in modern tomographic studies which reveal more and more details owing to their increasing resolution capabilities (e.g. Zielhuis and Nolet, 1994; Legendre et al., 2012; Schaeffer and Lebedev, 2013; Zhu and Tromp, 2013). However, details of the LAB topography and of properties of the SCLM in central Europe haven't been resolved by regional tomographic studies yet whereas local tomographic studies show higher resolution for smaller regions but do not provide regional images (e.g. Mathar et al., 2006) or do not resolve properties of the SCLM (e.g. Ritter et al., 2001).

To the south, the SCLM of central Europe is strictly bounded by the Alpine orogen. A crustal root reaching beyond 50 km depth has been

imaged by active seismic profiling, receiver functions and local earthquake tomography (e.g. Schmid et al., 1996; Schmid and Kissling, 2000). It was long assumed that the European lithosphere is southward subducting beneath the entire Alpine arc. A renewed discussion of the geodynamics of the Alpine collision was initiated by the tomographic model by Lippitsch et al. (2003) that clearly showed a north-ward directed subduction beneath the Eastern Alps, thus invoking the need for more detailed investigations of the deep structure below the orogen and its forelands, which is presently tackled by the pan-European AlpArray initiative (<http://www.seismo.ethz.ch/alparray>).

3. Surface wave tomography

The improved resolution of modern tomographic models owes strongly to the rapid increase in station coverage across the continent since the late 1990s, with methodological developments and increasing computational power facilitating the progress in models. With denser seismic networks, model parameterization (node spacing or cell sizes) can be reduced and resolution of the models significantly enhanced. To exploit these massive data volumes and their inherent information on the structure of the lithosphere, automated processing routines are required to extract observables from the waveform data which can be used for high-resolution seismic tomography. Surface wave phase velocities are particularly suited for lithospheric scale imaging as they can be measured with high accuracy over a large bandwidth which covers sensitivity from the shallow crust (<20 km, ~10 s period) to asthenospheric depths (>250 km, >200 s period) and their particularly sensitive to vertical variations in shear wave velocity, thus largely avoiding vertical smearing effects often present in investigations with body wave data.

In a recent study we have processed >1.3 million waveforms from >1000 seismic stations in central Europe and surroundings, performing >12 million individual inter-station phase velocity dispersion measurements (Soomro et al., 2016). After selection of smooth and reliable phase velocity curves with path-wise averaging we obtained a dataset of 63,000 inter-station Rayleigh wave phase velocity dispersion curves with an average standard error of <0.5%. From these accurate measurements we calculated and present in the following new isotropic Rayleigh wave phase velocity maps across central Europe. The estimated lateral resolution is about ~100 km (Soomro et al., 2016). The obtained coverage is indicated by Fig. 2.

At short (<20 s) period Rayleigh wave phase velocity sensitivity is restricted predominantly to the middle and lower crust, although strong anomalies in the shallow crust may be overprinting the maps. This is nicely seen in Fig. 3 at 12 s period, where the deep sedimentary cover in the Central European Basin System (CEBS) is expressed by very slow seismic velocities that cover an area from the North Sea to the Polish Basin. A comparison with sediment thickness (Scheck-Wenderoth and Lamarche, 2005) in the CEBS illustrates the resolving power of the presented maps. Sedimentary thickness contours align well with the outline of low velocity anomalies in the CEBS and, moreover, the amplitude of the anomaly is lowest in the North Sea, where the sediments reach thicknesses of >12 km. Towards the east, the sedimentary basin narrows in the Polish Basin (see 2500 m contour in Fig. 3) and the deep (>7500 m) depression within it appears less strong as compared to the North Sea. South of the CEBS there is no significant sedimentation (except for the deep Po basin south of the Alps) and faster velocities north of the Alps attribute to that. Along the Alpine and Carpathian Arc and in the Pannonian Basin slightly below average phase velocities are dominant with minimum values in the region of the Vienna Basin with <6 km sediments (e.g. Hölzel et al., 2008). For a comparison of short period surface wave phase velocities with sedimentary thickness in central Europe on a larger scale we refer to Soomro et al. (2016).

At 25 s period (Fig. 4) the most striking pattern is the clear separation between higher phase velocities in central and northern Europe from slower regions south of the Alpine Front (AF) and the convergence

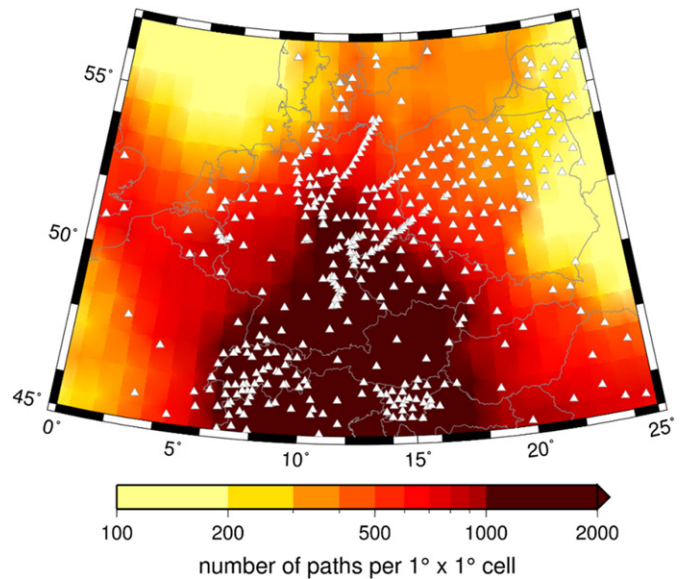


Fig. 2. Coverage of the surface wave tomography. Color coded is the number of paths per $1^\circ \times 1^\circ$ cells for a period of 55 s. White triangles indicate broad-band seismic stations. Note that the region outside is covered as well. The coverage is however lower there.

zone of Carpathian Arc and TTZ. Those variations can be largely related to variations in crustal thickness. Moho depths north of the Alps are known to vary only slightly around 30–35 km (e.g. Meissner and Rabbel, 1999) which is expressed by relatively faster velocities in the phase velocity map due to partial sensitivity to sub-Moho seismic velocities. This is particularly noteworthy since this “homogeneity” in Moho depth and sub-Moho velocities is opposed to the strong tectonic subdivision in top basement levels across the region. In the Alps, as well as along the central sections of the TTZ, crustal thickness reaches depths of >40 km (e.g. Grad and Tiira, 2009) leading to reduced surface wave phase velocities as the 25 s waves sense more crustal rocks. Towards the Carpathian-Pannonian System reduced velocities indicate that despite shallow crust, also variations in seismic velocities within the

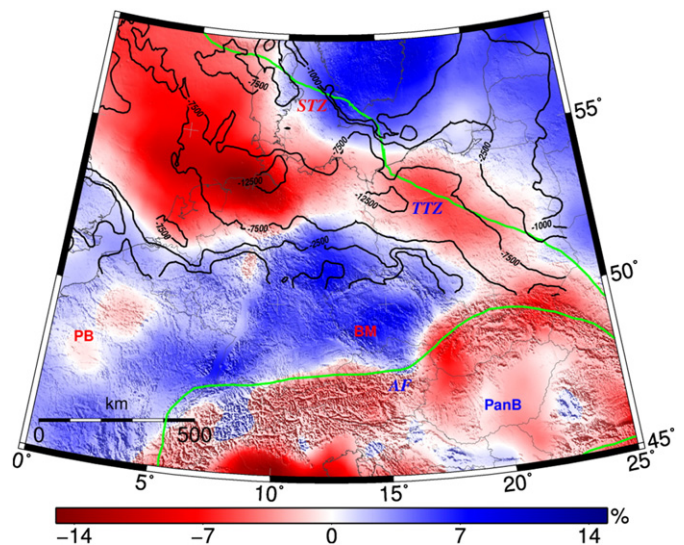


Fig. 3. Phase velocity map at 12 s period. Perturbations are shown in percent with respect to an average phase velocity of 3.21 km/s. The contours indicate sediment thickness in the Central European Basin System north of 50°N according to Scheck-Wenderoth and Lamarche (2005). AF: Alpine Front, BM: Bohemian Massif, PanB: Pannonian Basin, PB: Paris Basin, STZ: Sorgenfrei-Torquist Zone, TTZ: Tornquist-Teisseyre Zone.

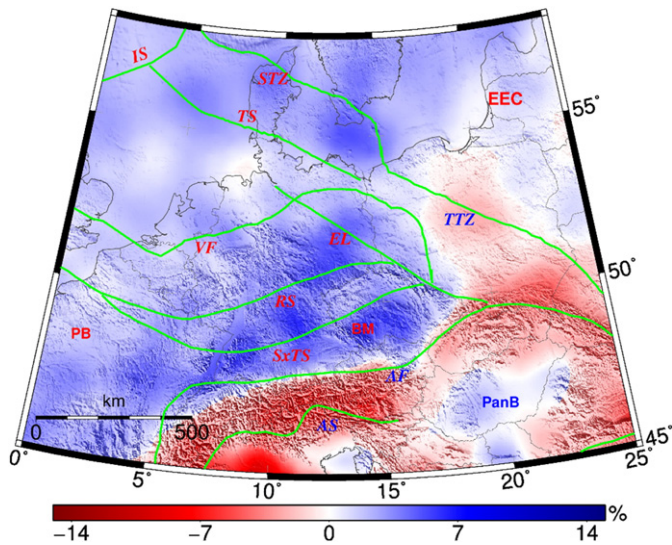


Fig. 4. Phase velocity map at 25 s period. Perturbations are shown in percent with respect to an average phase velocity of 3.7 km/s. AF: Alpine Front, AS: Alpine Suture, BM: Bohemian Massif, EL: Elbe Line, EEC: East European Craton, IS: Iapetus Suture, PanB: Pannonian Basin, PB: Paris Basin, RS: Rheic Suture, STZ: Sorgenfrei-Torquinst Zone, SxTS: Saxothuringian-Moldanubian Suture, TS: Thor Suture, TTZ: Tornquist-Teisseyre Zone, VF: Variscan Front.

crust (Carpathians) or effects of a shallow asthenosphere (Pannonian basin) influence the 25 s maps.

In Fig. 5 we present our 55 s period phase velocity map which is dominantly sensitive to variations in shear wave velocity at mantle lithospheric depths (70–120 km). Contrary to the shallowest mantle lithosphere, the mantle lithosphere is more heterogeneous at those depths. Faster than average velocities prevail in the northern part, most notably northeast of the Tornquist-Teisseyre Zone (TTZ) on the thick, old and cold mantle lithosphere of the East European Craton (EEC). Note also

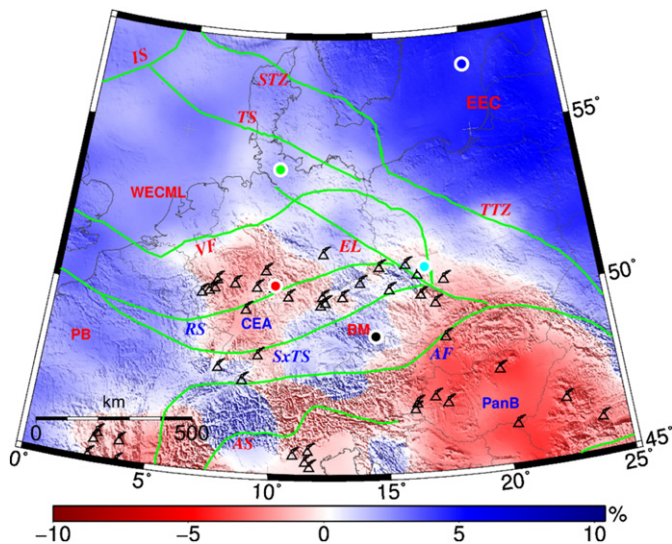


Fig. 5. Phase velocity map at 55 s period. Perturbations are shown in percent with respect to an average phase velocity of 3.98 km/s. Locations of Cenozoic volcanic fields are indicated by triangles. Colored dots mark locations of one-dimensional models given in Fig. 6. AF: Alpine Front, AS: Alpine Suture, BM: Bohemian Massif, black dot, CEA: Central European Asthenosphere, red dot, EEC: East European Craton, blue dot, EL: Elbe Line, IS: Iapetus Suture, PanB: Pannonian Basin, PB: Paris Basin, RS: Rheic Suture, STZ: Sorgenfrei-Torquinst Zone, SxTS: Saxothuringian-Moldanubian Suture, TS: Thor Suture, TTZ: Tornquist-Teisseyre Zone, WECML: Western European Continental Mantle Lithosphere, North German Basin: green dot, Polish Basin: cyan dot.

the sharp increase in seismic velocities across the TTZ east of 15°E. While velocities in the mantle lithosphere of the EEC are very fast, phase velocities in the WECML are still largely above average, although with reduced amplitude. South of the Variscan front, however, below average phase velocities seem to prevail which extend from the Rhenish Massif directly above the CEA indicated in Fig. 5 to the Alpine Foreland and to the Lower Rhine area to the northwest. This is consistent with previous observations of a shallow asthenosphere in central Europe (Central European Asthenosphere, CEA) beneath the Rhenish Massif, the Vogelsberg region and the upper Rhine graben (Ritter et al., 2001; Mathar et al., 2006; Legendre et al., 2012), although the lateral extent and confined contours of the CEA have been previously less clear compared to this map. Interestingly, the mantle lithosphere of the Bohemian Massif is surrounded by low velocities especially towards the NW in the region of the Eger Rift and towards the NE in Lower Silesia indicating a shallow asthenosphere also in those regions. Major properties of the LAB topography are obviously not related to Variscan structures (Fig. 5). This is an indication that the recent LAB topography is the result of post-Variscan processes.

In order to relate frequency dependent phase velocities more quantitatively to shear-wave velocities at depth we show in Fig. 6 inversion results for 5 selected representative locations. The locations are indicated in Fig. 5. In Fig. 6 the measured phase-velocity dispersion curves are given as assembled from phase velocity maps at 30 different frequencies between 8 s and 300 s (Soomro et al., 2016) together with uncertainties (grey areas). Broad-band Rayleigh wave dispersion curves are sensitive to shear-wave velocities at a broad depth range from the upper crust down to the upper mantle at about 300 km depth. The strong variability in phase velocities at short periods below about 20 s is due to the influence of crustal properties on the dispersion curves. Low phase velocities in the North German Basin (green) are caused by large sedimentary thicknesses. Between about 20 s and 200 s phase velocities are sensitive to properties of the mantle lithosphere and asthenosphere. Phase velocities in the EEC (blue) are significantly larger than in the Phanerozoic regions.

In Fig. 6 on the bottom the corresponding optimal one-dimensional shear-wave velocity models are given. They are obtained by an iterative gradient search algorithm following Meier et al. (2004). Velocities in the crust as well as the Moho depth are strongly damped towards the background models derived from the crustal model EuCRUST-07 (Tesauro et al., 2008). Below the Moho the background models follow the global ak135 model (Kennett et al., 1995, dashes line in Fig. 6). Model uncertainties are estimated from second derivatives around the optimal model (Meier et al., 2004). Note the overall very good consistency between measured phase velocities and synthetic curves for the optimal models (Fig. 6, top). Strong variations in shear-wave velocity up to about 8% are present in the uppermost mantle (Fig. 6, bottom). The presence of the asthenosphere beneath the Phanerozoic SCLM is clearly indicated by a strong reduction in the shear-wave velocity in all models expect in the model for the EEC (blue model in Fig. 6). Due to the smooth nature of the surface wave sensitivity kernels, the depth of the LAB is more difficult to estimate from inversion results of surface waves but can be approximately found in the middle of the zone where larger velocities within the SCLM decrease towards lower velocities in the asthenosphere (e.g. Bartzsch et al., 2011). The depth of the LAB can be estimated by inversion of accurate phase velocity measurements with an uncertainty of 10 km to 20 km for LAB depths lower than 100 km (Bartzsch et al., 2011). Differences in LAB depth are easier to resolve than absolute LAB depths by comparing the depth of the transition towards low velocities in the asthenosphere between models.

The about 250 km thick lithosphere of the East European Craton (blue model in Fig. 6) is in contrast to much lower lithospheric thicknesses in Phanerozoic central Europe (all other models in Fig. 6). The shallowest asthenosphere is found in central Europe (red model in Fig. 6) where phase velocities at intermediate periods are lower than average (Fig. 5). The significant reduction in the shear-wave velocity

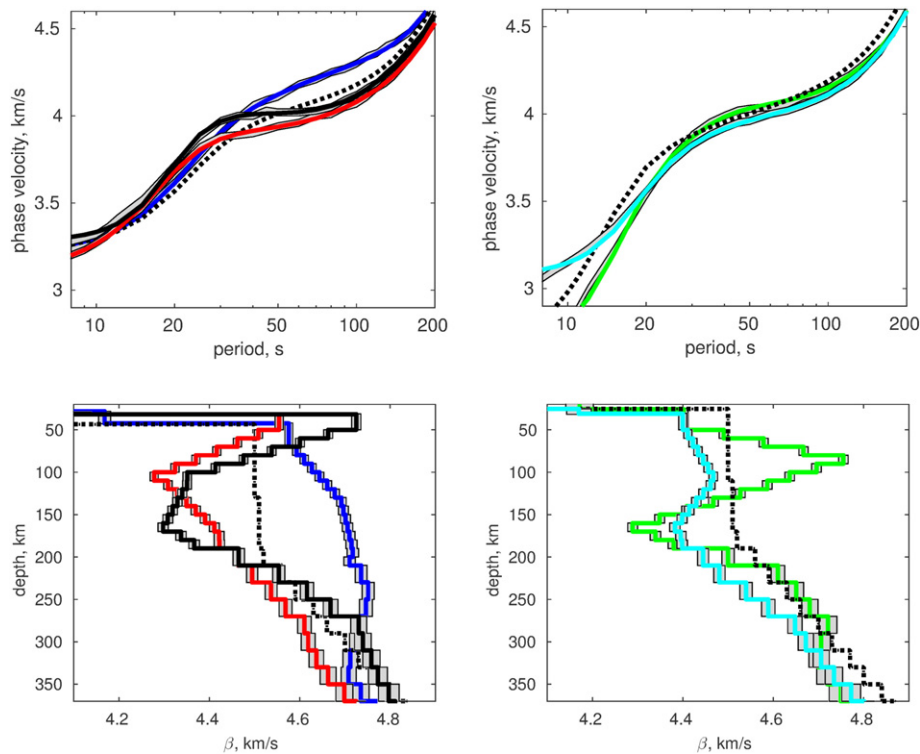


Fig. 6. (top) Phase velocities for optimal models at 5 selected locations. The grey areas show measured local phase velocities with uncertainties. The locations are indicated in Fig. 5 with the same colors as in Fig. 6. Bohemian Massif: black, Central European Platform: red, East European Craton: blue, North German Basin: green, Polish Basin: cyan. Dotted curves give the phase velocity for the background models for the EEC (left) and the NGB (right). (bottom) Optimal one-dimensional local shear-wave velocity models in the upper mantle resulting from the inversion of the dispersion curves together with estimated uncertainties (grey filled areas). Dotted lines indicate the background models for the EEC (left) and the NGB (right).

between about 70 km and 300 km depth is indicating the shallow asthenosphere in this region (Fig. 6). Beneath the Bohemian Massif the LAB is located about 20 km to 30 km deeper and the asthenosphere is found between about 90 km and 230 km depth (black model in Fig. 6). The mantle lithosphere in the North German Basin is clearly thicker (green model in Fig. 6) with a LAB depth of about 120 km. A similar LAB depth but much lower shear-wave velocities are found for the Polish Basin (cyan model in Fig. 6). Interestingly, beneath the Bohemian Massif and the North German Basin shear-wave velocities increase again significantly beneath the asthenosphere (black and green models in Fig. 6) indicating considerable heterogeneity in central Europe also below the asthenosphere.

Particularly the collocation of Cenozoic volcanism in central Europe with the extended low velocity anomaly is remarkable as it shows that the Cenozoic volcanism in central Europe occurs in regions with a thin lithosphere and a shallow asthenosphere (Fig. 5, Fig. 6). The lithosphere in these regions is thinned by up to about 40 km compared to the surroundings if a LAB depth of about 40 km to 60 km is assumed in the Eifel region (e.g. Mathar et al., 2006; Seiberlich et al., 2013 and Fig. 6) compared to LAB depths of about 100 km and larger beneath the CEBS, the Bohemian Massif and the Paris Basin (e.g. Babuška and Plomerová, 1992; Maystrenko and Scheck-Wenderoth, 2013 and Fig. 6). Remarkable is further that all regions with a thin lithosphere (<100 km) beneath continental regions in Europe are locations of Cenozoic intraplate volcanism (Legendre et al., 2012) indicating that a thinned lithosphere is a major prerequisite for the occurrence of anorogenic intraplate volcanism.

While the extended region of reduced seismic velocities in the Pannonian Basin at 55 s (Fig. 5) can be attributed to an overall shallow asthenosphere (Dando et al., 2011; Legendre et al., 2012), velocity anomalies in the Alps are of variable sign. In the western central Alps high velocities are indicative for subduction of the Eurasian plate towards the south beneath Adria. While in the east there are no

indications for a southward subduction in accordance to local body wave tomography (Lippitsch et al., 2003).

In Fig. 7 we compare the occurrence of the Rotliegend volcanics indicative for massive volcanism at about 290 Ma with Rayleigh wave

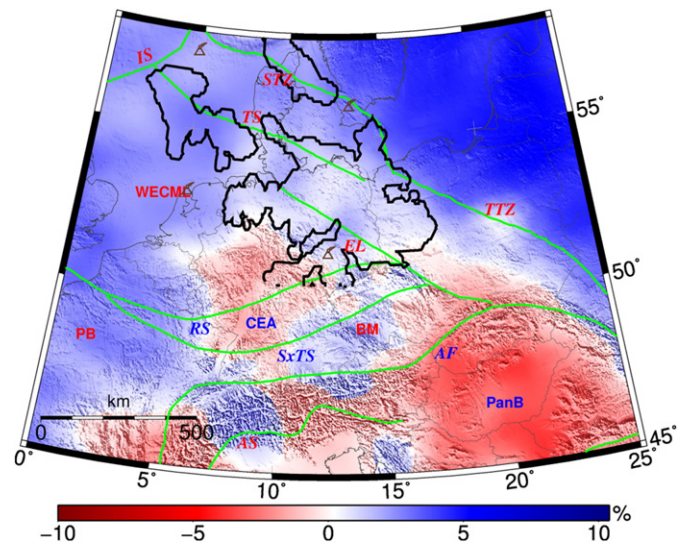


Fig. 7. Phase velocity map at 55 s period. Perturbations are shown in percent with respect to an average phase velocity of 3.98 km/s. Locations of Mesozoic volcanic fields (volcanoes) and the outline of the Rotliegend volcanics in the CEBS north of 50°N are indicated according to Scheck-Wenderoth and Lamarche (2005). AF: Alpine Front, AS: Alpine Suture, BM: Bohemian Massif, Central European Asthenosphere, EL: Elbe Line, IS: Iapetus Suture, PanB: Pannonian Basin, PB: Paris Basin, RS: Rhenic Suture, STZ: Sorgenfrei-Torquinst Zone, SxTS: Saxothuringian-Moldanubian Suture, TS: Thor Suture, TTZ: Tornquist-Teisseyre Zone, WECC: Western European Continental Mantle Lithosphere.

phase velocities at 55 s. While the Cenozoic volcanism is associated with a thin lithosphere (red model in Fig. 6) this is at present not the case for the Rotliegend volcanism in the area of the North German Basin (green model in Fig. 6). But it has to be assumed that at the time of the volcanism this area has been characterized by thermal heating from below and a thin lithosphere (van Wees et al., 2000). After the Rotliegend volcanism the North German Basin has been a site of almost continuous subsidence and sedimentation (e.g. Scheck-Wenderoth and Lamarche, 2005). This has been related to cooling of the mantle lithosphere (van Wees et al., 2000). Here we show that the area of the Rotliegend volcanics is indeed now a site of a rather normally thick continental lithosphere (green model in Fig. 6). This holds also for the sparse locations of Mesozoic volcanism in the area. We will discuss these observations further in Section 5.

4. Comparison to geochemical properties of the CECIP

In this section, we first review the geochemical properties of mafic magmas that form intraplate volcanic fields (cf. Section 1 and Fig. 1) which themselves form the Central European Cenozoic Igneous Province (CECIP) and compare them then to the tomographic images of the lithosphere-asthenosphere system. The mafic rocks in the volcanic fields of the CECIP are almost exclusively silica-undersaturated mafic volcanics such as melilitites, nephelinites, basanites and alkalic basalts. Primary tholeiitic basalts are restricted to the Vogelsberg volcanic field (Jung and Masberg, 1998; Bogaard and Wörner, 2003). Silica-saturated rocks in other fields, e.g., Rhön and Hessian Depression, are products of crustal assimilation as indicated by their isotope characteristics (Wedepohl, 1985; Jung and Hoernes, 2000). Additionally, a number of fields of smaller eruptive volumes occur in southern Germany mainly bound to graben systems: Odenwald (Schmitt et al., 2007), Kaiserstuhl and Hegau (Keller, 2008), Urach (Hegner et al., 1995). Within these fields strongly silica-undersaturated mafic rocks dominate (e.g., melilitites (U), melilite-nephelinites, basanites and nephelinites, incl. carbonatitic differentiates. The age of the magmas is either Late Cretaceous (O: 68 Ma) or Miocene (K, H, U: 16–11 Ma).

In the northern transect of the CECIP from the Eifel to NW Bohemia/Vogtland the Miocene to recent magmas on average exhibit increasing Si-saturation and decreasing REE enrichment (indicated by decreasing $(La/Yb)_N$ -ratios) approaching the volcanic field of the Vogelsberg volcanic field. Alkalic to tholeiitic basalts only erupted during the first pulse of activity in the Vogelsberg volcanic field (16–19 Ma) while melilitite bearing nephelinites or melilitites only occur in the Vogtland to the east or in the Quaternary Eifel volcanic fields to the west. The Vogelsberg volcanic field is located at the crossing of the CECIP with the northern extension of the Paleogene Upper Rhine graben structure (Ziegler, 1994). Based on experimental data by Green (1972) and Green and Falloon (1998) the chemical variations from melilitites to tholeiitic basalts can be modelled as the result of (1) an increasing degree of partial melting from 2% to some 15% (values are readjusted based on the REE melting model explained in Haase et al., 2004) combined with increasing melt proportions of the shallower spinel-lherzolite (<2 GPa) instead of the garnet-lherzolite mantle source, as well as (2) shallower equilibration depths of melt segregation approaching the elongation of the Upper Rhine graben structure. The isotopic uniformity of the those mafic volcanics in the CECIP without crustal assimilation indicates a uniform, primarily depleted and secondarily slightly enriched, amphibole-bearing mantle source throughout the transect, independent of the time of eruption (Abratis et al., 2007; Kolb et al., 2012; Jung et al., 2012). Only east of the Bohemian Massif the mantle source differs as is indicated by isotopic heterogeneity of the mafic magmas in Lower Silesia (Ladenberger et al., 2004).

Within the Bohemian Massif the chemical variations in the igneous melts indicate an overprint during melt generation by two lithosphere penetrating NNW-running tectonic structures paralleling the Tornquist-Teisseyre Lineament: (1) along the Labe (Elbe) Zone (No.

13 in Table 1), (2) along the zone of recent earthquake swarms crossing the Ohre Rift in the Cheb Basin (No. 12). Approaching these structures the Si-saturation of mafic magmas decreases to melilitite-bearing compositions (Ulrych et al., 2008). According to REE melting models the amount of partial mantle melting is reduced and the depth of melt separation increased to >90 km (Dasgupta et al., 2007; Green, 1972; Wilson et al., 1995), which is indicated by a strong HREE depletion in the rocks (Abratis et al., 2009). As the volume of erupted magma is reduced as well, the melting environment is similar to that at oceanic fracture zones. This may possibly be explained by the cooling effect of these tectonic elements on the melting zone or by metasomatically induced linear lithospheric mantle heterogeneities (e.g. MgCa-carbonates) (Brey, 1978; Abratis et al., 2009) possibly corresponding to paleo plate boundaries (Babuska et al., 2007).

In Fig. 8 the location of analyzed volcanic fields is compared to the phase velocity map at 55 s that is strongly sensitive to variations in the LAB depth between about 70 km to 120 km. Obviously, the volcanic fields occur in regions of a shallow asthenosphere as seen by seismic velocities or at its rim. The latter means that volcanic activity is often found above transitions from deeper to shallower asthenosphere. This supports the suggestion e.g. by Lebedev et al. (2006) that intraplate volcanism is caused by decompressional melting of mantle material flowing from deeper levels beneath regions of a thick plate towards regions of a shallow LAB. The collocation of volcanic fields and low velocities in the upper mantle beneath the CECIP has already been noted by Hoernle et al. (1995) using a low resolution tomographic model available at that time. They related the intraplate volcanism to an upwelling mantle. Similarly, Ritter et al. (2001) found evidence for low velocities in the upper mantle beneath the volcanic fields of the Eifel and Vogelsberg regions. Our tomographic images support the findings that the volcanic activity is located above upper mantle regions with low velocities; we relate however the location of the intraplate volcanism of the CECIP to LAB topography.

As shown in Fig. 6 and discussed in Section 3, low velocities in Fig. 8 indicate a shallow LAB. Low velocities may be caused by high temperatures or by the presence of fluids. These are the two variables that Ritter et al. (2001) use to explain the characteristics of the so-called Eifel plume. While an excess temperature of 100–150 °C are taken as causes to explain the P-wave velocities being reduced by 1–2%, partial melt in an OH-bearing metasomatised lithospheric mantle are thought to

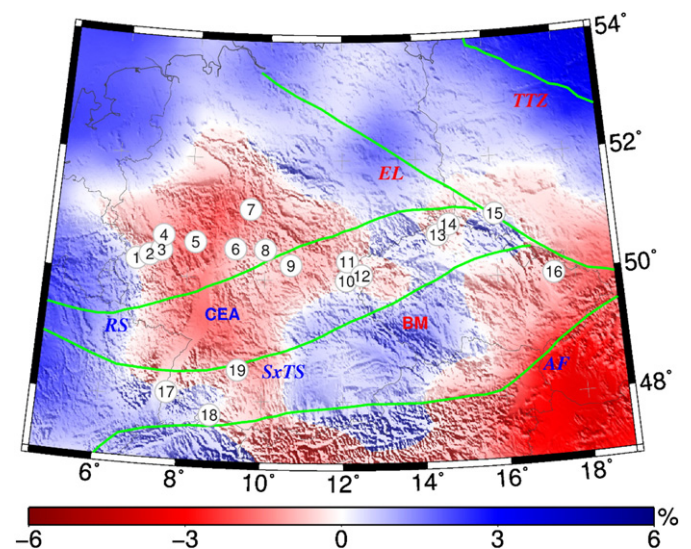


Fig. 8. Location of the analyzed volcanic fields of the CECIP (Table 1) plotted on top of the phase velocity map at 55 s. AF: Alpine Deformation Front, BM: Bohemian Massif, CEA: Central European Asthenosphere, EL: Elbe Line, RS: Rheic Suture, SxTS: Saxothuringian-Moldanubian Suture, TTZ: Tornquist-Teisseyre Zone. The numbering of the volcanic fields refers to Table 1.

cause the 5% reduction of S-wave velocities. From a shallow LAB imaged by seismic methods we can however not conclude that immediately below this seismic LAB mantle material with a MORB source composition possibly enriched by deep plume material is present. Instead below the seismic LAB a mixture of heated lithospheric mantle and mantle material intruded from below is present. This model is deduced to explain the major and trace element as well as isotope characteristics of the alkaline lavas in the CECIP: while the primitive mantle normalized negative K-anomalies require amphibole as OH-bearing mineral in a metasomatically enriched lithospheric source, the HIMU-component in the isotope ratios is taken as evidence for the asthenospheric component (e.g., Kolb et al., 2012; Schubert et al., 2015). However, the latter argument is not conclusive as the HIMU component is as well present in hydrated SCLM xenoliths (Witt-Eickschen et al., 2003; Witt-Eickschen, 2007).

In Fig. 9 we show the spatial distribution of the average partial melting, the SiO_2 content of the melts, the average temperature of the magma generation, and the depth of the magma generation. Also the age of the latest volcanic eruption in the considered volcanic fields is given. First, there is no evidence for a spatial migration of volcanic activity or a hot spot track within the CECIP. With respect to time, the volcanic activity shows a rather random distribution. It started about 70 Ma ago, showed the strongest activity at about 15 Ma and is obviously ongoing. Furthermore, the degree of partial melting, the temperature and the depth of melt generation show a remarkable spatial variability with the tendency that the strongest activity with highest temperatures and lowest depths of melt generation occurring in the center of the LAB upwelling in the Vogelsberg region. Contrarily, at the rim of the shallow asthenosphere melt generation tends to occur at deeper levels, lower temperatures, lower partial melting, and low SiO_2 content. Melt generation seems to be scattered between the current shallow LAB depth and a depth of about 100 km – approximately the thickness of the plate in the surroundings of the shallow LAB. The spatial variability of the geochemical properties of the volcanic fields rules out the presence of a large single magma reservoir beneath the CECIP. These observations may be explained by intrusion of hot mantle material into the SCLM causing the seismically imaged LAB to rise. Rejuvenation of the SCLM is accompanied by intrusion of hot mantle material from below resulting in

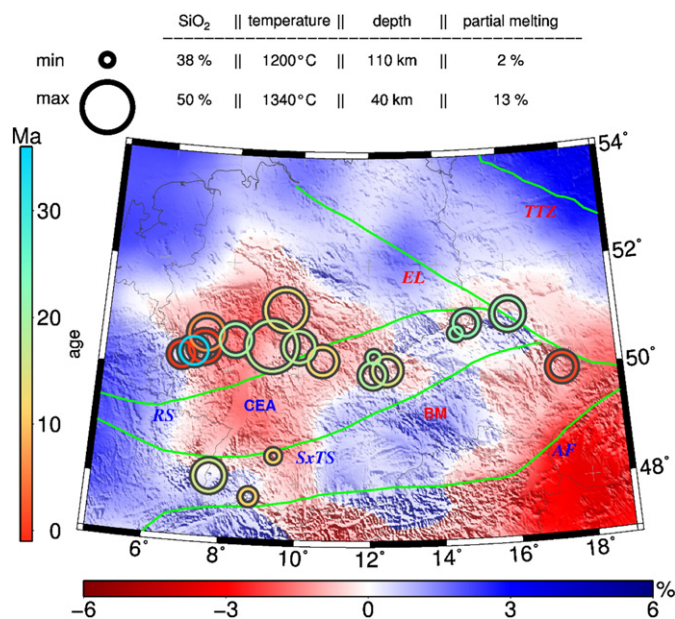


Fig. 9. Average degree of partial melting, average SiO_2 content, average temperature and depth of magma generation in the volcanic fields of the CECIP (size of the circles) plotted on top of the phase velocity map at 55 s. The color of the circle indicates the age of the latest activity.

distributed partial melting and mixing with heated and partially melted former SCLM. We can rule out simple end member models of either a complete replacement of the SCLM by hot sublithospheric mantle (possibly by plume material) as well as a simple buckling of the SCLM with only conductive heating from below. The uplifted seismic LAB marks the transition between the more or less intact SCLM above and heated lithospheric mantle material with intrusions and scattered nests of partial melting below. We conclude that thermal erosion of the SCLM accompanied by uplift and volcanic activity is the result of heating by intrusion of sublithospheric mantle as indicated in Fig. 10.

The evolution of the subcontinental lithospheric mantle in central Europe can be further constraint by analyzing mantle xenoliths found in the CECIP. Only those from a few fields (Eifel, Lower Hessa, Rhoen, and Massif Central) have been studied in detail (Stosch and Lugmair, 1986; Downes and Dupuy, 1987; Stosch, 1987; Witt and Seck, 1989; Kramm and Wedepohl, 1990; Rudnick and Goldstein, 1990; Witt-Eickschen and Kramm, 1998; Downes, 2001; Witt-Eickschen et al., 2003). The least modified xenoliths seem to be light rare earth (LREE) depleted protoliths with a Paleoproterozoic depletion age of ~2 Ga (Stosch, 1987). A subsequent multistage enrichment and depletion history prior to 1.1 Ga must be deduced for some peridotite xenoliths based on their Pb isotope composition (Stosch and Lugmair, 1986). The majority of xenoliths experienced a large-scale metasomatic modification in consequence of presumably the Hercynian subduction (Downes, 2001). Evidence for such an event is provided by Sr, Nd, and Pb isotope characteristics in granulitic xenoliths (Rudnick and Goldstein, 1990). Witt and Seck (1989) deduced from textural evidence that this metasomatic event was associated with lithospheric deformation. Lu-Hf data from unveined xenoliths imply a resetting of the isotope system by an event <200 Ma (Thiemens and Sprung, 2015). Based on textural, geochemical and Sr-Nd-isotope evidence this event must have occurred sometime prior to the Cenozoic volcanism (Witt-Eickschen et al., 1998), presumably by melt infiltration during the early Cretaceous (Wilson et al., 1995). Beneath the Eifel common additional vein mineralisations are associated with the Cenozoic volcanism (Witt-Eickschen et al., 1998).

5. Post-Permian evolution of the SCLM in central Europe

The evolution of the lithosphere in the Eifel and the upper Rhine Graben regions as well as of the CECIP have been subject of a number of studies (e.g. Ziegler, 1990, 1994, 2002; Scheck and Bayer, 1999; van Wees et al., 2000; Dèzes et al., 2004; Brink, 2005; Scheck-Wenderoth

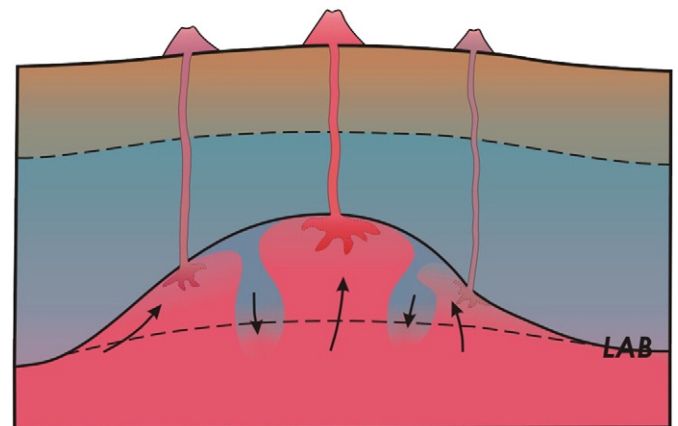


Fig. 10. Sketch of the model for the uplift of the lithosphere-asthenosphere boundary (LAB) in the Central European Cenozoic Igneous Province (CECIP). The lower dashed line indicates the LAB before thermal erosion of SCLM. The solid line indicates the recent LAB upwelling as inferred from seismic observations. Below the recent LAB heated SCLM is mixing with upwelling asthenospheric mantle. The upper dashed line indicates the Moho.

and Lamarche, 2005; Ziegler and Dèzes, 2006). Also the response of the lithosphere to external tectonic forces since the late Cretaceous has been investigated (e.g. Cloetingh et al., 1999; Marotta et al., 2002; Mazur et al., 2005; Kley and Voigt, 2008). In contrast to the Variscan assembly of central Europe there are however no regional large-scale models for the Post-Permian evolution of the lithosphere available. In this section and in Fig. 11 we sketch the evolution of the lithosphere in central Europe from the lower Permian onwards based on geological evidence in order to explain the current state of the SCLM as imaged by seismic tomography. We discuss the data presented here in the context of an evolutionary model that can be tested against all available observations from surface evolution, tectonic crustal structure, and the variations of Central European volcanism in space and time. In some cases, the possible conclusions are rather obvious, in other cases, e.g. regarding the volcanism near the SW margin of the Baltic Shield, in the North German Basin and in the North Sea, a simple correlation between the former thermal state of the upper mantle and volcanism is less easy to establish.

As discussed in the previous sections, intraplate volcanic activity is a manifestation of increased heat flow from below the SCLM, and therefore occurs in regions with a thin lithosphere. This is now the case in the region of the CECIP, and has to be inferred also for the time of the volcanic activity in the CEBS in Lower Permian times. After cessation of the volcanic activity there, cooling of the lithosphere caused a density and thickness increase, resulting in subsidence and sedimentation. Seismic tomography shows that the lithosphere in this region is about 100 km thick today. Thus, the LAB of the continental lithosphere may be a dynamic boundary, similar to the LAB of the oceanic plates. The evolution of the Phanerozoic SCLM in central Europe is inferred based on the following arguments: (1) Large-scale subsidence indicated by sedimentation without strong extension is interpreted as evidence for cooling of the lithosphere and for an increase of the lithospheric thickness. (2) The presence of intra-plate volcanism is taken as evidence for a shallow asthenosphere and a thin plate. (3) Large-scale uplift without strong compression is interpreted as evidence for a rise of the LAB and a thinning of the lithosphere. (4) Small-scale topography is assumed to result mainly from deformation of the brittle upper crust or erosion. The schematic NNE–SSW oriented profile in Fig. 11 reaches from the southern margin of the East European Craton (EEC) towards the Alps, crossing the North German Basin (NGB) and the CECIP. The thickness of the EEC is assumed to be almost constant in time with a thickness of about 250 km.

5.1. State of the lithosphere after the Variscan orogeny

There is much evidence in the literature that the areas underlying the central European Platform (CEP) and the NGB were made of normally thick or even thin continental crust (e.g. Meissner and Bortfeld, 1990; Aichroth et al., 1992). The presence of abundant granitic plutons and widespread laminated lower crust (see upper image in Fig. 11) can be interpreted as a consequence of a thickened Variscan orogenic crust collapsing by the end of the Carboniferous (e.g. Franke and Oncken, 1990; Franke, 2006). This process was accompanied by widespread migmatite formation (e.g. Tanner and Behrmann, 1995) and/or mylonitization and shearing (e.g. Krohe and Eisbacher, 1988), magmatic underplating, or a mixture of these processes (e.g. Meissner et al., 2006). Below the crust–mantle boundary the tectonic processes driving the changes to the crustal structure may have been lithospheric delamination and asthenospheric upwelling (e.g. Schott and Schmeling, 1998; Arnold et al., 2001). This prompted the widespread volcanism and further crustal extension in the lower Permian, and defines the “starting model” for the lithospheric evolution in central Europe in the Mesozoic and Cenozoic (Fig. 11a).

Furthermore, the laterally rather homogeneous SCLM found by DSS and our tomographic studies (Legendre et al., 2012; Soomro et al., 2016) is consistent with the SCLM in the region of the Variscan and Caledonian orogenies forming, or at least getting strongly deformed and homogenized, after terrane collision. This implies, further, a post-Permian age of large parts of the current SCLM in central Europe. Our findings also support the suggestion by Meissner et al. (1991) that the seismic signature of the lower parts of the lithosphere in central Europe, including the lower crust and the lithospheric mantle, are effectively younger than that of the brittle upper crust. The high-velocity lower crust in the region of the NGB may have been very likely formed by intrusions in the lower Permian (Rabbel et al., 1995).

5.2. Cooling as indicated by Mesozoic basin subsidence and sedimentation

After the cessation of extensive volcanism in the Permian, the area of the NGB developed as a shallow-water, epicontinental basin, while most of the southern part of the CEP remained above sea level. By the beginning of the Triassic, terrestrial or shallow marine sedimentation prevailed throughout (see Fig. 11b), in response to slow and continuous basin subsidence. The most straightforward way to explain this subsidence in terms of tectonic processes is continuous freezing of mantle lithosphere to the base of the continental crust in central Europe. As stated above, the evolution of the LAB may have progressed as a dynamic feature akin to that beneath oceanic plates. This leads to a total average thermal subsidence in the order of two or three kilometers over about 100 Ma – a fact that can be accounted for in the sedimentary records at least of the major basins (e.g. Ziegler, 1990; van Wees et al., 2000; Scheck-Wenderoth and Lamarche, 2005).

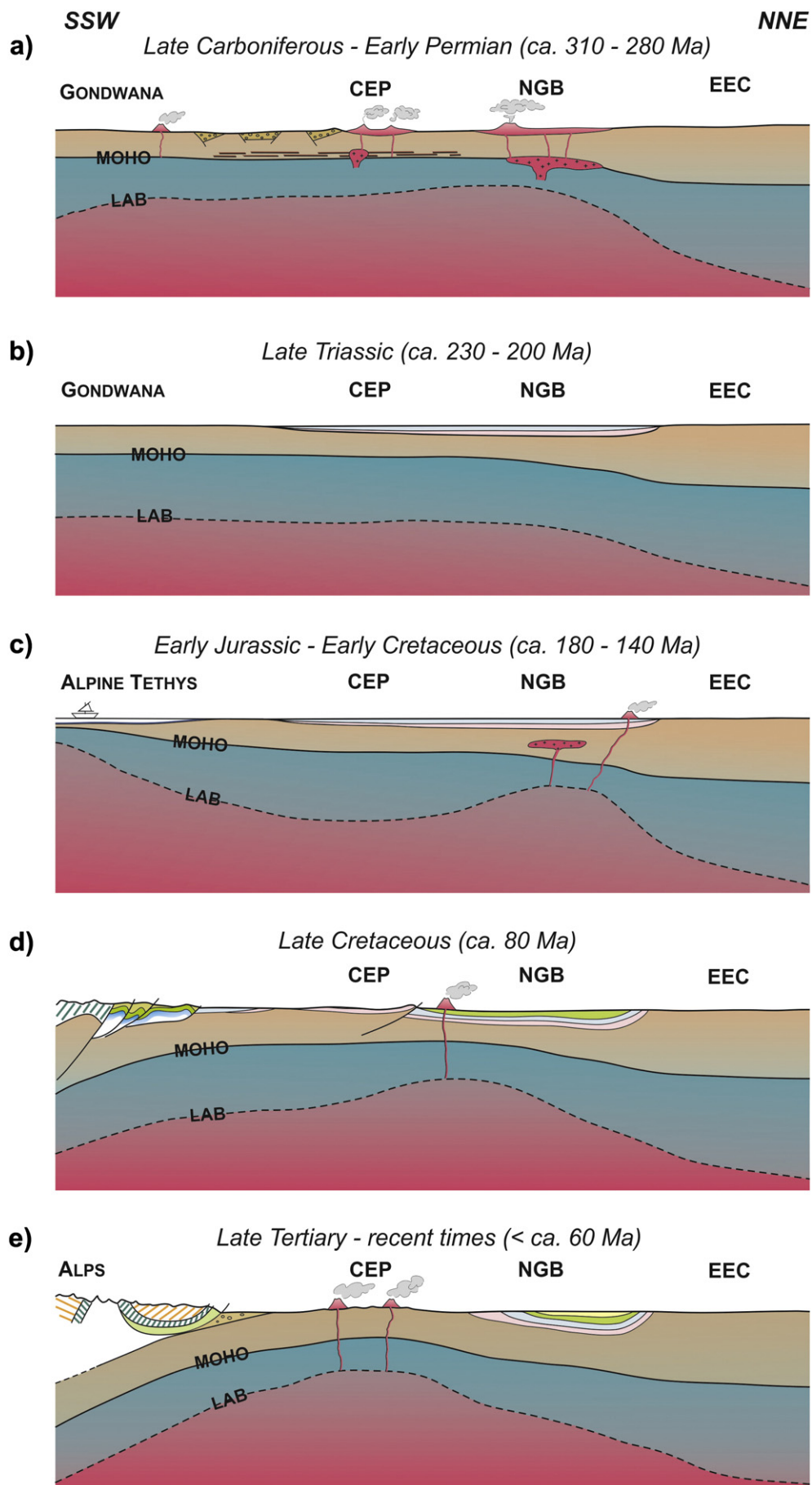
From the Early Jurassic onwards (Fig. 11c) basin subsidence continues, with the exception of the southeastern part of the CEP, where the sedimentary record is very condensed or even punctuated, especially in the surroundings of the Bohemian Massif (see 1000 m isopach of sediment thickness in Fig. 3). In most parts, however, sedimentation is not interrupted, especially in the NGB. South of the CEP, made up of the Bohemian Massif and the South German Platform, sedimentation becomes more and more pelagic through time, in response to the evolution of the Tethyan passive margin through the Jurassic and the Cretaceous with basin carbonates and predominantly fine clastics. This development is best depicted in the Helvetic units of Switzerland, and, to a lesser extent, in Austria (e.g. Faupl and Wagreich, 1992; Lihou and Allen, 1996; Behrmann and Tanner, 2006). Subsidence at the southern margin of the CEP, thus, is more related to crustal and lithospheric stretching, and less to a signal of asthenospheric upwelling.

5.3. Reappearance of volcanism in the northern study area in the Jurassic and Cretaceous

What is special in the northern part of the study area is the appearance of magmatic rocks in the NGB, the North Sea, and the boundary zone to the Eastern European Platform (Fig. 11c). This magmatism is enigmatic, mainly because it appeared in a large number of areas (Skåne, Forties, Egersund Basin, Northern Germany, Northern North Sea; see e.g. Furnes et al., 1982; Ritchie et al., 1988; Bergelin, 2009; Bergelin et al., 2011) and lasted for a long time, mainly culminating in three phases (c. 180–160 Ma, 145 Ma, 110 Ma), and producing overall very limited amounts of melt. The concept of a pluton beneath the NGB in the area of Bramsche is interesting and controversial (e.g. discussion in Brink, 2013), but has found wide support in the geophysical and sedimentological literature, explaining anomalous diagenesis in overlying sediments.

In some of the cases there is evidence for these melts resulting from minimum melting of hydrated upper mantle peridotites (see discussion

Fig. 11. Sketch of the Mesozoic and Cenozoic evolution of the SCLM in central Europe. See text for further discussions. CEP: Central European Platform, EEC: East European Craton, LAB: Lithosphere–Asthenosphere Boundary, NGB: North German Basin.



in Bergelin et al., 2011). So, this type of intraplate magmatism is probably not related to a thermal upwelling, but more likely a reflection of melting prompted by ponded fluids at the base of the lithosphere. It is not easy to imagine the origin of such fluids, but they could be remains of detached hydrated lithospheric slabs, be it from the Caledonian or the Variscan orogenies. More discussion of this idea can be found in Bergelin et al. (2011).

On the other hand sedimentation in the CEBS has been widely interrupted in the Jurassic (e.g. Scheck and Bayer, 1999; Hansen et al., 2005; Scheck-Wenderoth and Lamarche, 2005) supporting the view that the volcanism in the area has been associated with some regional-scale uplift at the surface and an upwelling of the LAB (Fig. 11c).

5.4. Compressional tectonics, Upper Cretaceous

Fig. 11d shows that the CEP and NGB areas were subjected to more subsidence in the northern part, and – especially in the Upper Cretaceous – to compressive tectonics (e.g. Mazur et al., 2005). The associated N-S shortening probably relates to the beginning Alpine convergent orogeny (left in the fourth drawing, Fig. 11). It should be borne in mind that – although creating impressive structures like the Harz Boundary Fault, the Frankonian Line (Fig. 1) and many other fault structures, the overall shortening strains are relatively minor, and probably did not contribute much to the lithospheric thickening. In contrast, a rather strong lithosphere has been suggested for the NGB because the inversion focused on the southern and to a lesser extent on the northern margins of the basin whereas there is little evidence for internal deformation in the axial parts of the basin (Mazur et al., 2005). This is consistent with the recent normal or even enlarged lithospheric thickness in the region (Fig. 6). Interestingly, there was considerable deformation in the axial part of the Polish Basin indicating a rather weak rheology of the lithosphere. This may correspond to the low shear-wave velocities in the SCLM in this region (Fig. 6).

5.5. Evolution since the Tertiary and current state of the lithosphere

Fig. 11e illustrates the discussion that is included in the descriptive part of this paper (Section 3). In terms of tectonics it is important to note that the evolution of the European Cenozoic Rift System (Ziegler, 2002) and widespread volcanism coincide in space and time, but do so only very broadly. As a rift system, the structure is only weakly magmatic, and seems to resemble more a passive rift. Where volcanism is observed it is often younger than the rifting initiation (e.g. Upper Rhine Graben; Fig. 1), and localization of the magmas appear more as a consequence of deformation than the other way round. Large parts of the system are also distinctly non-magmatic, like the Northern Rhine Embayment or the North Sea (Fig. 1). This strongly supports our inference that it is mantle processes that influence the LAB changes beneath the CEP and the NGB. It is likely that the LAB has been uplifted in central Europe during the Cenozoic coeval with the volcanism and the uplift. The low lithospheric thickness and the large amount of uplift of the LAB in the region of the CECIP cannot be explained by pure buckling of the lithosphere due to inversion tectonics. Also, sublithospheric mantle currently found at depth between the recent LAB and about 100 km is the result of melting of a formerly thicker SCLM and intrusions by mantle material from larger depths. This is consistent with a larger thickness of the lithosphere before the Late Cretaceous. First evidence for volcanic activity in the CECIP and incipient uplift is found at about 80 Ma. These observations yield constraints for the age of the shallow asthenosphere in central Europe: it has been developed since about this time.

Also in the region of Mesozoic volcanism the lithosphere shows today a thickness of about 80 km to 120 km implying cooling and thickening of the SCLM north of the CECIP in the Cenozoic. Further to the northeast, the lithosphere beneath the North Sea has been thinned by extension at that time.

It is interesting to note in Fig. 11 the southward migration of the region of intraplate volcanism and thinned Phanerozoic lithosphere through time since the Early Jurassic. This may be related to the northward movement of the Eurasian plate over a thermal anomaly anchored in the mantle below. Alternatively, asthenospheric flow guided by LAB topography and caused by the convergence and subduction of Adria and Eurasia in the Alpine region since the Upper Cretaceous may have played a role. The variability of the Phanerozoic LAB with time may be further enhanced by proximity to margins of cratonic lithosphere, where hot material may flow upwards from under the thick lithosphere beneath cratons towards the shallower LAB depth beneath surrounding continental mantle lithosphere and where deformable Phanerozoic continental lithosphere is in contact with stable cratonic lithosphere.

A deeper source for the mantle upwelling has to be assumed in the first scenario whereas an asthenosphere confined to shallower depths flowing beneath the SCML would be present in the second scenario. To distinguish between these scenarios or a mixture of both, high resolution tomographic images of the Eurasian mantle below 300 km as well as images of seismic anisotropy indicating asthenospheric flow are needed.

6. Conclusions

Surface-wave tomography using automated measurements of Rayleigh wave phase velocities with all currently available data yields phase-velocity maps in broad period ranges, sampling S-wave velocities at various depths, from shallow crustal structures (including sedimentary basins) to the lower crust and the Moho, to the SCLM, and to the asthenosphere below. We observe that (1) the lithosphere is thinner in regions of Cenozoic intraplate volcanism in the CECIP compared to regions with no Cenozoic volcanism; (2) the lower SCLM of the Bohemian Massif is surrounded to the west, north, and northeast by asthenospheric mantle; (3) an about 100–120 km thick lithosphere is found beneath the North German Basin southwest of the STZ; (4) the SCLM in central Europe appears to be rather homogeneous and its present isotropic-average, seismic-velocity structure does not show any contrasts across the Caledonian and Variscan terrane boundaries that are mapped at the surface.

A remarkable correlation between geochemical properties of volcanic fields in the CECIP and the topography of the LAB in central Europe is found: high melting rates, high silica contents, high temperatures and low depths of magma generation are found preferably in regions of low lithospheric thicknesses and vice versa. Furthermore, there is geochemical evidence that magma in the CECIP has not been generated in pure sublithospheric mantle. Indications for melting of the SCLM can be found. Therefore, low lithospheric thicknesses observed in central Europe at present are a result of melting of the SCLM and intrusion of sublithospheric mantle into the SCLM in the Cenozoic.

Beneath the North German Basin, the LAB is found currently at depths of about 100 km to 120 km. Thus, the lithosphere in the region of nearly continuous subsidence and sedimentation since the Permian is significantly thicker than beneath the low mountain ranges of the CECIP. Remarkably, in the region of thicker lithosphere thick layers of Rotliegend volcanics are present indicating a thermal impulse and low lithospheric thicknesses at this earlier time. These observations point to temporal changes of the LAB depth in central Europe and highlight the dynamic nature of the Phanerozoic continental LAB. The presence of relatively thick lithosphere in the region of the North German Basin is consistent with subsidence and sedimentation there being caused by the cooling of continental lithosphere and an increase of the LAB depth. The synthesis of tomographic results with geological and geochemical evidence results in a generic model for the Mesozoic and Cenozoic evolution of the continental lithosphere in central Europe.

The model developed by Meissner and coworkers for central Europe, with a brittle upper crust that has preserved the imprint of pre- and syn-orogenic deformation and overlays a lower crust with a nearly flat Moho

and a seismic structure indicating post-collisional deformation and intrusions, can be extended to the SCLM showing a variable thickness in time and space due to the influence of post-orogenic processes. This model may be applicable to the post-collisional evolution of the Phanerozoic SCLM in regions beyond central Europe, for example the Aegean or Anatolia, where a largely new SCLM has probably formed beneath the crust assembled by nappe stacking and terrane accretion.

Acknowledgement

We thank M. Scheck-Wenderoth for making available to us her compilation of the sedimentary thicknesses in the North German Basin. R.S. was funded by German Science Foundation grant ME 1320/4-1. S.L. was supported, in part, by Science Foundation Ireland (grant 13/CDA/2192). We thank three anonymous reviewers for their constructive criticism.

References

- Abramovitz, T., Thybo, H., 2000. Seismic images of Caledonian, lithosphere-scale collision structures in the southeastern North Sea along Mona Lisa profile 2. *Tectonophysics* 317, 27–54.
- Abratis, M., Mädlér, J., Hautmann, S., Leyk, H.-J., Meyer, R., Lippolt, J., Viereck-Götte, L., 2007. Two distinct Miocene age ranges of basaltic rocks from the Rhön and Heldburg areas (Germany) based on $^{40}\text{Ar}/^{39}\text{Ar}$ step heating data. *Geochemistry* 67, 133–150.
- Abratis, M., Munsel, D., Viereck-Götte, 2009. Melilitite und Melilitit-führende Magmatite des sächsischen Vogtlands: Petrographie und Mineralchemie. *Z. Geol. Wiss.* 37, 41–79 (Berlin).
- Aichroth, B., Prodehl, C., Thybo, H., 1992. Crustal structure along the central segment of the EGT from seismic-refraction studies. *Tectonophysics* 207, 43–64.
- Alsina, D., Snieder, R., 1996. Constraints on the velocity structure beneath the Tornquist-Teisseyre Zone from beam-forming analysis. *Geophys. J. Int.* 126, 205–218.
- Arnold, J., Jacoby, W.R., Schmeling, H., Schott, B., 2001. Continental collision and the dynamic and thermal evolution of the Variscan orogenic crustal root – numerical models. *J. Geodyn.* 31, 273–291.
- Artemieva, I.M., Meissner, R., 2012. Crustal thickness controlled by plate tectonics: a review of crust–mantle interaction processes illustrated by European examples. *Tectonophysics* 530–531, 18–49.
- Artemieva, I.M., Thybo, H., Kaban, M.K., 2006. Deep Europe today: geophysical synthesis of the upper mantle structure and lithospheric processes over 3.5 Ga. *Geol. Soc. Lond. Mem.* 32, 11–41.
- BABEL Working Group, 1991. Deep seismic survey images crustal structure of Tornquist Zone beneath southern Baltic Sea. *Geophys. Res. Lett.* 18, 1091–1094.
- BABEL Working Group, 1993. Deep seismic reflection/refraction interpretation of crustal structure along BABEL profiles A and B in the southern Baltic Sea. *Geophys. J. Int.* 112, 243–325.
- Babuška, V., Plomerová, J., 1992. The lithosphere in central Europe – seismological and petrological aspects. *Tectonophysics* 207, 141–163.
- Babuska, V., Plomerova, J., Fischer, T., 2007. Intraplate seismicity in the western Bohemian Massif (central Europe): a possible correlation with a paleoplate junction. *J. Geodyn.* 44, 149.
- Babuška, V., Plomerová, J., Šílený, J., 1984. Spatial variations of P residuals and deep structure of the European lithosphere. *Geophys. J. R. Astron. Soc.* 79, 363–383.
- Badura, J., Pěcskay, Z., Koszowska, E., Wolska, A., Zuchiewicz, W., Przybylski, B., 2005. New age and petrological constraints on Lower Silesian basalts, SW Poland. *Acta Geodyn. Geomater.* 2 (3), 7–15, 139.
- Bartzsch, S., Lebedev, S., Meier, T., 2011. Resolving the lithosphere-asthenosphere boundary with seismic Rayleigh waves. *Geophys. J. Int.* <http://dx.doi.org/10.1111/j.1365-246X.2011.05096.x>.
- Becker, T.W., Conrad, C.P., Schaeffer, A.J., Lebedev, S., 2014. Origin of azimuthal seismic anisotropy in oceanic plates and mantle. *Earth Planet. Sci. Lett.* 401, 236–250.
- Behrmann, J.H., Tanner, D.C., 2006. Structural synthesis of the Northern Calcareous Alps, TRANSALP segment. *Tectonophysics* 414, 225–240.
- Bergelin, I., 2009. Jurassic volcanism in Skåne, southern Sweden, and its relation to coeval regional and global events. *GFF* 131, 165–175. <http://dx.doi.org/10.1080/11035890902851278>.
- Bergelin, I., Obst, K., Söderlund, U., Larsson, K., Johansson, L., 2011. Mesozoic rift magmatism in the North Sea region: $^{40}\text{Ar}/^{39}\text{Ar}$ geochronology of Scania basalts and geochemical constraints. *Int. J. Earth Sci.* 100, 787–804. <http://dx.doi.org/10.1007/s00531-010-0516-3> (*Geol. Rundsch.*).
- Berthelsen, A., 1992. From Precambrian to Variscan Europe. In: Blundell, D., Freeman, R., Mueller, S. (Eds.), *A Continent Revealed: The European Geotraverse*. Cambridge University Press, Cambridge, pp. 153–164.
- Bijwaard, H., Spakman, W., 2000. Non-linear global P-wave tomography by iterated linearized inversion. *Geophys. J. Int.* 141, 71–82.
- Bird, P., 1979. Continental delamination and the Colorado Plateau. *J. Geophys. Res.* 84 (B13), 7561–7571.
- Blusztajn, J., Hart, S.R., 1989. Sr, Nd, and Pb isotopic character of tertiary basalts from southwest Poland. *Geochim. Cosmochim. Acta* 53, 2689–2696.
- Bogaard, P.J.F., Wörner, G., 2003. Petrogenesis of basaltic to tholeiitic volcanic rocks from the Miocene Vogelsberg, Central Germany. *J. Petrol.* 44 (3), 569–602.
- Boschi, L., Fry, B., Ekström, G., Giardini, D., 2009. The European Upper Mantle as Seen by Surface Waves. *Surveys in Geophysics*. 30. Springer, Netherlands, pp. 463–501.
- Bowring, S.A., Williams, I.S., 1999. Priscoan (4.00–4.03 Ga) orthogneisses from northwestern Canada. *Contrib. Mineral. Petrol.* 134 (1), 3–16.
- Brey, G., 1978. Origin of olivine melilitites – chemical and experimental constraints. *J. Volcanol. Geotherm. Res.* 3, 61–88.
- Brey, G., Keller, J., 1982. Hegau volcanic province. *Excurs. Guide*, 3. Intern. Kimberlite Conf. 1982, Clermont-Ferrand.
- Brink, H.-J., 2005. The evolution of the North German Basin and the metamorphism of the lower crust. *Int. J. Earth Sci.* 94, 1103–1116. <http://dx.doi.org/10.1007/s00531-005-0037-7> (*Geol. Rundsch.*).
- Brink, H.-J., 2013. Die Intrusion von Bramsche – ein Irrtum im invertierten Niedersächsischen Becken? *Z. Dtsch. Ges. Geowiss.* 164, 33–48. <http://dx.doi.org/10.1127/1860-1804/2013/0011>.
- Bruneton, M., Pedersen, H., Farra, V., Arndt, N., Vacher, P., Achauer, U., Alinaghi, A., Ansorge, J., Bock, G., Friederich, W., Grad, M., Guterch, A., Heikkinen, P., Hjelt, S.-E., Hyvoenen, T., Ikonen, J.-P., Kissling, E., Komminaho, K., Korja, A., Kozlovskaya, E., Nevky, M., Paulssen, H., Pavlenkova, N., Plomerova, J., Raita, T., Riznichenko, O., Roberts, R., Sandoval, S., Sanina, I., Sharov, N., Shomali, Z., Tiikainen, J., Wielandt, E., Wilegalla, K., Yliniemi, J., Yurov, Y., 2004. Complex lithospheric structure under the Central Baltic Shield from surface wave tomography. *J. Geophys. Res.* 109 (B10). <http://dx.doi.org/10.1029/2003JB002947>.
- Büchner, J., Tietz, O., Viereck, L., Suhr, P., Abratis, M., 2015. Volcanology, geochemistry and age of the Lausitz Volcanic Field. *Int. J. Earth Sci.* <http://dx.doi.org/10.1007/s00531-015-1165-3>.
- Budweg, M., Bock, G., Weber, M., 2006. The Eifel Plume – imaged with converted seismic waves. *Geophys. J. Int.* 166, 579–589.
- Cajz, V., Schnabl, P., Pěcskay, Z., Skácelová, Z., Venhodová, D., Šlechtá, S., Čížková, K., 2012. Chronological implications of the paleomagnetic record of the Late Cenozoic volcanic activity along the Moravia-Silesia border (NE Bohemian Massif). *Geol. Carpath.* 63 (5), 423–435.
- Calcagnile, G., 1982. The lithosphere-asthenosphere system in Fennoscandia. *Tectonophysics* 90, 19–35.
- Cloetingh, S., Burov, E., Poliakov, A., 1999. Lithosphere folding: primary response to compression? (from Central Asia to Paris Basin). *Tectonics* 18. <http://dx.doi.org/10.1029/1999TC009040>.
- Cloetingh, S.A.P.L., Ziegler, P.A., Bogaard, P.J.F., Andriessen, P.A.M., Artemieva, I.M., Bada, G., Van Balen, R.T., Beekman, F., Ben-Avraham, Z., Brun, J.P., Bunge, H.P., 2007. TOPO-EUROPE: the geoscience of coupled deep Earth-surface processes. *Glob. Planet. Chang.* 58, 1–118.
- Condie, K.C., 1998. Episodic continental growth and supercontinents: a mantle avalanche connection? *Earth Planet. Sci. Lett.* 163 (1), 97–108.
- Cotte, N., Pedersen, H.A., 2002. Sharp contrast in lithospheric structure across the Sorgenfrei-Tornquist Zone as inferred by Rayleigh wave analysis of TOR1 project data. *Tectonophysics* 360, 75–88.
- Dando, B.D.E., Stuart, G.W., Houseman, G.A., Hegedüs, E., Brückl, E., Radovanović, S., 2011. Teleseismic tomography of the mantle in the Carpathian–Pannonian region of central Europe. *Geophys. J. Int.* 186, 11–31.
- Dasgupta, R., Hirschmann, M.M., Smith, N.D., 2007. Partial melting experiments of peridotite + CO₂ at 3 GPa and genesis of Alkaline Ocean island basalts. *J. Petrol.* 48 (11), 2093–2124.
- Davis, E.E., Lister, C.R.B., 1974. Fundamentals of ridge crest topography. *Earth Planet. Sci. Lett.* 21, 405–413.
- Debayle, E., Ricard, Y., 2012. A global shear velocity model of the upper mantle from fundamental and higher Rayleigh mode measurements. *J. Geophys. Res.* 117, B10308. <http://dx.doi.org/10.1029/2012JB009288>.
- Dèzes, P., Schmid, S.M., Ziegler, P.A., 2004. Evolution of the European Cenozoic Rift system: interaction of the Alpine and Pyrenean orogens with their foreland lithosphere. *Tectonophysics* 389, 1–33.
- Downes, H., 2001. Formation and modification of the shallow subcontinental lithospheric mantle: a review of geochemical evidence from ultramafic xenolith suites and tectonically emplaced ultramafic massifs of western and central Europe. *J. Petrol.* 42, 233–250.
- Downes, H., Dupuy, C., 1987. Textural, isotopic and REE variations in spinel peridotite xenoliths, Massif Central, France. *Earth Planet. Sci. Lett.* 82, 121–135.
- EUGENO-S working group, 1988. Crustal structure and tectonic evolution of the transition between the Baltic Shield and the North German Caledonides (the EUGENO-S project). *Tectonophysics* 150, 253–348.
- Faupl, P., Wagreich, M., 1992. Cretaceous flysch and pelagic sequences of the Eastern Alps – correlations, heavy minerals, and paleogeographic implications. *Cretac. Res.* 13, 387–403.
- Fekiacova, Z., Mertz, D.F., Hofmann, A.W., 2007b. Geodynamic setting of the tertiary Hoheifel Volcanism (Germany), part II: geochemistry and Sr, Nd and Pb isotopic compositions. In: Ritter, R., Christensen, U. (Eds.), *Mantle Plumes. A Multidisciplinary Approach*. Springer-Verlag, Berlin Heidelberg, pp. 207–240.
- Fekiacova, Z., Mertz, D.F., Renne, P.R., 2007a. Geodynamic setting of the tertiary Hoheifel Volcanism (Germany), part I: $^{40}\text{Ar}/^{39}\text{Ar}$ geochronology. In: Ritter, R., Christensen, U. (Eds.), *Mantle Plumes. A Multidisciplinary Approach*. Springer-Verlag, Berlin Heidelberg, pp. 185–206.
- Foley, S.F., 2008. Rejuvenation and erosion of the cratonic lithosphere. *Nat. Geosci.* 1, 503–510.
- Franke, W., 2006. The Variscan orogen in Central Europe: construction and collapse. *Geol. Soc. Lond. Mem.* 32, 333–343.
- Franke, W., Oncken, O., 1990. Geodynamic evolution of the North-Central Variscides – a comic strip. In: Freeman, R., Giese, P., Mueller, S. (Eds.), *The European Geotraverse: Integrative Studies*. European Science Foundation, Strasbourg, pp. 187–194.
- French, S., Lekic, V., Romanowicz, B., 2013. Waveform tomography reveals channelled flow at the base of the oceanic asthenosphere. *Science* 342 (6155), 227–230.

- Furnes, H., Elvsborg, A., Malm, O.A., 1982. Lower and Middle Jurassic alkaline magmatism in the Egersund Sub-Basin, North Sea. *Mar. Geol.* 46, 53–69.
- Geissler, W.H., Sodoudi, F., Kind, R., 2010. Thickness of the central and eastern European lithosphere as seen by S receiver functions. *Geophys. J. Int.* 181, 604–634.
- Geyer, O.F., Gwinner, M.P., 1984. Die Schwäbisch Alb und ihr Vorland. Sammlung Geologische Führer 67. Gebrüder Bornträger, Berlin-Stuttgart.
- Goes, S., Govers, R., Vacher, P., 2000. Shallow mantle temperatures under Europe from P and S wave tomography. *J. Geophys. Res.* 105, 11153–11169.
- Grad, M., Tiira, T., 2009. The Moho depth map of the European Plate. *Geophys. J. Int.* 176, 279–292.
- Grad, M., Guterch, A., Polkowska-Purys, A., 2005. Crustal structure of the Trans-European Suture Zone in Central Poland—re-interpretation of the LT-2, LT-4 and LT-5 deep seismic sounding profiles. *Geol. Quart.* 49, 243–252.
- Grand, S.P., 2002. Mantle shear-wave tomography and the fate of subducted slabs. *Philosophical Transactions of the Royal Society of London A: Mathematical, Physical and Engineering Sciences* 360. The Royal Society, pp. 2475–2491.
- Grand, S., van der Hilst, R., Widiyantoro, S., 1997. Global seismic tomography: a snapshot of convection in the earth. *GSA Today* 7 (4), 1–7.
- Green, D.H., 1972. Magmatic activity as the major process in the chemical evolution of the earth's crust and mantle. In: Ritsema, A.R. (Ed.), *The Upper Mantle*. Tectonophysics 13, pp. 47–71.
- Green, D.H., Falloon, T.J., 1998. Pyrolyte: a Ringwood concept and its current expression. In: Jackson, I. (Ed.), *The Earth's Mantle – Composition, Structure, and Evolution*. Cambridge University Press, pp. 311–378.
- Gregersen, S., Voss, P., Nielsen, L., Achauer, U., Busche, H., Rabbel, W., Shomali, Z., 2010. Uniqueness of modeling results from teleseismic P-Wave tomography in Project Tor. *Tectonophysics* 481, 99–107.
- Gurnis, M., Davies, G.F., 1986. Apparent episodic crustal growth arising from a smoothly evolving mantle. *Geology* 14 (5), 396–399.
- Haase, K.M., Renno, A.D., 2008. Variation of magma generation and mantle sources during continental rifting observed in Cenozoic lavas from the Eger Rift, Central Europe. *Chem. Geol.* 257, 192–201.
- Haase, K.M., Goldschmidt, B., Garbe-Schoenberg, C.D., 2004. Petrogenesis of Tertiary continental intra-plate lavas from the Westerwald region, Germany. *J. Petrol.* 45, 883–905.
- Hansen, M.B., Lykke-Andersen, H., Dehghani, A., Gajewski, D., Hübscher, C., Olesen, M., Reicherter, K., 2005. The Mesozoic–Cenozoic structural framework of the Bay of Kiel area, western Baltic Sea. *Int. J. Earth Sci.* 94, 1070–1082. <http://dx.doi.org/10.1007/s00531-005-0001-6> (Geol Rundsch).
- Hawkesworth, C.J., Dhuime, B., Pietranik, A.B., Cawood, P.A., Kemp, A.I.S., Storey, C.D., 2010. The generation and evolution of the continental crust. *J. Geol. Soc.* 167 (2), 229–248.
- Hegner, E., Walter, H.J., Satir, M., 1995. Pb–Sr–Nd isotope compositions and trace element geochemistry of megacrysts and melilitites from the Tertiary Urach volcanic field: source composition of small volume melts under SW Germany. *Contrib. Mineral. Petrol.* 122, 322–335.
- Hoernle, K., Zhang, Y.-S., Graham, D., 1995. Seismic and geochemical evidence for large-scale mantle upwelling beneath the eastern Atlantic and Western and Central Europe. *Nature* 374, 34–39.
- Hölzel, M., Wägreich, M., Faber, R., Strauss, F., 2008. Regional subsidence analysis in the Vienna Basin (Austria). *Austrian J. Earth Sci.* 101, 88–98.
- Huckenholz, H.G., Büchel, G., 1988. Tertiärer Vulkanismus der Hoheifel. Exkursion C 1, DMG-Tagung 1988. *Fortschr. Mineral.* 66, 43–82, Bb. 2.
- Huckenholz, H.G., Schröder, B., 1985. Tertiärer Vulkanismus im bayrischen Teil des Eger Grabens und des mesozoischen Vorlandes. *Jber. Mitt. oberrhein. geol. Ver. N.F.* 67 pp. 107–124.
- Huckenholz, H.G., Werner, C.D., 1990. Die tertiären Vulkanite der Heldburger Gangschar (Bayerisch-thüringisches Grabfeld). *Berichte der Deutschen Mineral. Ges.* 2, 1–42.
- Jordan, T.H., 1975. The continental tectosphere. *Rev. Geophys.* 13, 1–12.
- Jordan, T.H., 1988. Structure and formation of the continental tectosphere. *J. Petrol.* (1), 11–37 (Special Lithosphere Issue).
- Jung, S., Hoernes, S., 2000. The major- and trace-element and isotope (Sr, Nd, O) geochemistry of Cenozoic mafic volcanic rocks from the Rhön area (Central Germany): petrology, mantle source characteristics and implications for asthenosphere–lithosphere interactions. *J. Volcanol. Geotherm. Res.* 99, 27–53.
- Jung, S., Masberg, P., 1998. Major- and trace-element systematics and isotope geochemistry of Cenozoic mafic volcanic rocks from the Vogelsberg (Central Germany) Constraints on the origin of continental alkaline and tholeiitic basalts and their mantle source. *J. Volcanol. Geotherm. Res.* 86, 151–177.
- Jung, C., Jung, S., Hoffer, E., Berndt, J., 2006. Petrogenesis of Tertiary mafic alkaline magmas in the Hoheifel, Germany. *J. Petrol.* 47, 1637–1671.
- Jung, S., Pfänder, J.A., Brüggemann, G., Stracke, A., 2005. Sources of primitive alkaline volcanic rocks from the Central European Volcanic Province (Rhön, Germany) inferred from Hf, Os and Pb isotopes. *Contrib. Mineral. Petrol.* 150, 546–559.
- Jung, S., Vieten, K., Romer, R.L., Mezger, K., Hoernes, S., Satir, M., 2012. Petrogenesis of Tertiary alkaline magmas in the Siebengebirge, Germany. *J. Petrol.* 53, 2381–2409.
- Keller, J., 2008. Tertiary Rhinegraben Volcanism: Kaiserstuhl und Hegau. 9th International Kimberlite Conference in Frankfurt/Main, Germany. August 2008. Field Trip Guide. pp. 1–38 (with contributions by S. Spürghin and T. Weissenberger).
- Kennett, B.L.N., Engdahl, E.R., Buland, R., 1995. Constraints on seismic velocities in the Earth from traveltimes. *Geophys. J. Int.* 122, 108–124.
- Khan, A., Boschi, L., Connolly, J.A.D., 2011. Mapping the Earth's thermochemical and anisotropic structure using global surface wave data. *J. Geophys. Res. Solid Earth* 116, B01301.
- Kind, R., Sodoudi, F., Yuan, X., Shomali, H., Roberts, R., Gee, D., Eken, T., Bianchi, M., Tilmann, F., Balling, N., Jacobsen, B., Kumar, P., Geissler, W., 2013. Scandinavia – a former Tibet? *Geochim. Geophys. Geosyst.* 14, 4479–4487.
- Klemperer, S.L., Matthews, D.H., 1987. Iapetus suture located beneath the North Sea by BIRPS deep seismic reflection profiling. *Geology* 15, 195–198.
- Kley, J., Voigt, T., 2008. Late Cretaceous intraplate thrusting in central Europe: effect of Africa–Iberia–Europe convergence, not Alpine collision. *Geology* 36, 839–842. <http://dx.doi.org/10.1130/G24930A.1>.
- Knapmeyer-Endrun, B., Krüger, F., Legendre, C., Geissler, W., 2013. Tracing the influence of the Trans-European Suture Zone into the mantle transition zone. *Earth Planet. Sci. Lett.* 363, 73–87.
- Kolb, M., Paulick, H., Kirchenbaur, M., Münker, C., 2012. Petrogenesis of mafic to felsic lavas from the Oligocene Siebengebirge Volcanic Field (Germany): implications for the origin of intracontinental volcanism in Central Europe. *J. Petrol.* 53, 2349–2379.
- Kramm, U., Wedepohl, K.H., 1990. Tertiary basalts and peridotite xenoliths from the Hessian Depression (NW Germany) reflecting mantle compositions low in radiogenic Nd and Sr. *Contrib. Mineral. Petrol.* 106, 1–8.
- Krohe, A., Eisbacher, G.H., 1988. Oblique crustal detachment in the Variscan Schwarzwald, southwestern Germany. *Geol. Rundsch.* 77, 25–43.
- Krüger, J.C., Romer, R.L., Kämpf, H., 2013. Late Cretaceous ultramafic lamprophyres and carbonatites from the Delitzsch Complex, Germany. *Chem. Geol.* 353, 140–150.
- Ladenberger, A., Michalik, M., Tomek, C., Peate, D.W., 2004. Major, trace elements characteristics and isotopic compositions of tertiary volcanic rocks from SW Poland. In: Loren, M.W., Zagadzon, P.P. (Eds.), *International Workshop “Basalt 2004”. Abstracts Volume & Excursion Guide*, Warocław, pp. 17–18.
- Lebedev, S., van der Hilst, R.D., 2008. Global upper-mantle tomography with the automated multimode inversion of surface and S-wave forms. *Geophys. J. Int.* 173, 505–518.
- Lebedev, S., Meier, T., van der Hilst, R., 2006. Asthenospheric flow and origin of volcanism in the Baikal rift area. *Earth Planet. Sci. Lett.* <http://dx.doi.org/10.1016/j.epsl.2006.07.007>.
- Legendre, C.P., Meier, T., Lebedev, S., Friederich, W., Viereck-Götte, L., 2012. A shear wave velocity model of the European upper mantle from automated inversion of seismic shear and surface waveforms. *Geophys. J. Int.* 191, 282–304.
- Levshin, A.L., Schweitzer, J., Weidle, C., Shapiro, N.M., Ritzwoller, M.H., 2007. Surface wave tomography of the Barents Sea and surrounding regions. *Geophys. J. Int.* 170, 441–459.
- Lihou, J.C., Allen, P.A., 1996. Importance of inherited rift margin structures in the early North Alpine Foreland Basin, Switzerland. *Basin Res.* 8, 425–442.
- Lippitsch, R., Kissling, E., Ansorge, J., 2003. Upper mantle structure beneath the Alpine orogen from high-resolution teleseismic tomography. *J. Geophys. Res.* 108 (B8), 2376–2390.
- Lippolt, H.J., Todt, W., 1978. Isotopische Alterbestimmungen an Vulkaniten des Westerwaldes. *N. Jb. Geol. Paläont. (Monatsh.)* 6, 332–352.
- Lustrino, M., Wilson, M., 2007. The circum-Mediterranean anorogenic Cenozoic igneous province. *Earth Sci. Rev.* 81, 1–65. <http://dx.doi.org/10.1016/j.earscirev.2006.09.002>.
- Marotta, A.M., Bayer, U., Thybo, H., Scheck, M., 2002. Origin of the regional stress in the North German basin: results from numerical modelling. *Tectonophysics* 360, 245–264.
- Marquering, H., Snieder, R., 1996. Shear-wave velocity structure beneath Europe, the northeastern Atlantic and western Asia from waveform inversions including surface-wave mode coupling. *Geophys. J. Int.* 127, 283–304.
- Masters, G., Laske, G., Bolton, H., Dziewonski, A., 2000. The relative behavior of shear velocity, bulk sound speed, and compressional velocity in the mantle: implications for chemical and thermal structure Earth's deep interior: mineral physics and tomography from the atomic to the global scale. *Am. Geophys. Union* 63–87.
- Mathar, J.P., Ritter, J.R.R., Friederich, W., 2006. Surface waves image the top of the Eifel plume. *Geophys. J. Int.* 164, 377–382.
- Maupin, V., Agostini, A., Artemieva, I., Balling, N., Beekman, F., Ebbing, J., England, R., Frassetto, A., Gradmann, S., Jacobsen, B., Köhler, A., Kvarven, T., Medhus, A., Mjelde, R., Ritter, J., Sokoutis, D., Stratford, W., Thybo, H., Wawerzinek, B., Weidle, C., 2013. The deep structure of the Scandes and its relation to tectonic history and present-day topography. *Tectonophysics* 602, 15–37.
- Maystrenko, Y., Scheck-Wenderoth, M., 2013. 3D lithosphere-scale density model of the Central European Basin System and adjacent areas. *Tectonophysics* 601, 53–77.
- Mazur, S., Scheck-Wenderoth, M., Krzywiec, P., 2005. Different modes of the Late Cretaceous–Early Tertiary inversion in the North German and Polish basins. *Int. J. Earth Sci.* 94, 782–798 (Geol. Rundsch.).
- McCann, T., 2008. *The Geology of Central Europe, Volume 2: Mesozoic and Cenozoic*. Geological Society, London.
- McKenzie, D., 1978. Some remarks on the development of sedimentary basins. *Earth Planet. Sci. Lett.* 40, 25–32.
- McKenzie, D., Jackson, J.A., Priestley, K., 2005. Thermal structure of oceanic and continental lithosphere. *Earth Planet. Sci. Lett.* 233 (3–4), 337–349.
- Meier, T., Dietrich, K., Stöckert, B., Harjes, H.-P., 2004. One-dimensional models of shear-wave velocity for the eastern Mediterranean obtained from the inversion of Rayleigh wave phase velocities and tectonic implications. *Geophys. J. Int.* 156, 45–58.
- Meissner, R., 1999. Terrane accumulation and collapse in central Europe: seismic and rheological constraints. *Tectonophysics* 305, 93–107.
- Meissner, R., Bortfeld, R.K., 1990. DEKORP Atlas. Springer Verlag, Berlin, Heidelberg (80 pp).
- Meissner, R., Rabbel, W., 1999. Nature of crustal reflectivity along the DEKORP profiles in Germany in comparison with reflection patterns from different tectonic units worldwide: a review. *Pure and Applied Geophysics* 156. Birkhäuser-Verlag, pp. 7–28.
- Meissner, R., Tanner, B., 1993. From collision to collapse: phases of lithospheric evolution as monitored by seismic records. *Phys. Earth Planet. Inter.* 79, 75–86.
- Meissner, R., Rabbel, W., Kern, H., 2006. Seismic lamination and anisotropy of the lower continental crust. *Tectonophysics* 416, 81–99.

- Meissner, R., Wever, T., Sadowiak, P., 1991. Continental collisions and seismic signature. *Geophys. J. Int.* 105, 15–23.
- Mertes, H., Schmincke, H.-U., 1985. Mafic potassic lavas of the Quaternary West Eifel volcanic field 1: major and trace elements. *Contrib. Mineral. Petrol.* 89, 330–345.
- Meyer, R., Abratis, M., Viereck-Götte, L., Mädler, J., Hertogen, J., Romer, R.L., 2002. Mantelquellen des Vulkanismus in der thüringischen Rhön. *Beitr. Geol. Thüringen* 9, 75–105.
- MONA LISA Working Group, 1997. MONA LISA: deep seismic investigations of the lithosphere in the southeastern North Sea. *Tectonophysics* 269, 1–19.
- Müller, R.D., Sdrolias, M., Gaiña, C., Roest, W.R., 2008. Age, spreading rates, and spreading asymmetry of the world's ocean crust. *Geochem. Geophys. Geosyst.* 9 (4).
- Nolet, G., Zielhuis, A., 1994. Low S Velocities Under the Tornquist-Teisseyre Zone: Evidence for Water Injection Into the Transition Zone by Subduction. *Journal of Geophysical Research: Solid Earth*. 99 pp. 15813–15820.
- Olsson, S., Roberts, R.G., Boethvarsson, R., 2007. Analysis of waves converted from S to P in the upper mantle beneath the Baltic Shield. *Earth Planet. Sci. Lett.* 257, 37–46.
- Pedersen, H., Debayle, E., Maupin, V., 2013. Strong lateral variations of lithospheric mantle beneath cratons – example from the Baltic Shield. *Earth Planet. Sci. Lett.* 2013 (383), 164–172.
- Peter, D., Boschi, L., Deschamps, F., Fry, B., Ekström, G., Giardini, D., 2008. A new finite-frequency shear-velocity model of the European-Mediterranean region. *Geophys. Res. Lett.* 35, L16315.
- Pharaoh, T.C., 1999. Palaeozoic terranes and their lithospheric boundaries within the Trans-European Suture Zone (TESZ): a review. *Tectonophysics* 314, 17–41.
- Plomerova, J., Babuska, V., Vecsey, L., Koubá, D., 2002. Seismic anisotropy of the lithosphere around the Trans-European Suture Zone (TESZ) based on teleseismic body-wave data of the TOR experiment. *Tectonophysics* 360, 89–114.
- Poudjom Djomani, Y.H., O'Reilly, S.Y., Griffin, W.L., Morgan, P., 2001. The density structure of subcontinental lithosphere through time. *Earth Planet. Sci. Lett.* 184, 605–621.
- Rabbel, W., Forste, K., Schulze, A., Bittner, R., Rohi, J., Reichert, J.C., 1995. A high-velocity layer in the lower crust of the North German Basin. *Terra Nova* 7, 327–337.
- Rickers, F., Fichtner, A., Trampert, J., 2013. The Iceland-Jan Mayen plume system and its impact on mantle dynamics in the North Atlantic region: evidence from full-waveform inversion. *Earth Planet. Sci. Lett.* 367, 39–51.
- Ritchie, J.D., Swallow, J.L., Mitchell, J.G., Morton, A.C., 1988. Jurassic ages from intrusives and extrusives within the Forties Igneous Province. *Scott. J. Geol.* 24, 81–88.
- Ritsema, J., Deuss, A., van Heijst, H.J., Woodhouse, J.H., 2011. S4ORTS: a degree-40 shear-velocity model for the mantle from new Rayleigh wave dispersion, teleseismic traveltime and normal-mode splitting function measurements. *Geophys. J. Int.* 184, 1223–1236.
- Ritter, J.R.R., Jordan, M., Christensen, U.R., Achauer, U., 2001. A mantle plume below the Eifel volcanic fields, Germany. *Earth Planet. Sci. Lett.* 186, 7–14.
- Ritzwoller, M.H., Levshin, A.L., 1998. Eurasian surface wave tomography: group velocities. *J. Geophys. Res.* 103, 4839–4878.
- Rohrmüller, J., Horn, P., Peterek, A., Teipel, U., 2005. Specification of the excursion stops – first day: geology and structure of the lithosphere. Introduction. In: Kämpf, H., Peterek, A., Rohrmüller, J., Kumpel, H.-J., Geissler, W.H. (Eds.), *The KTB Deep Crustal Laboratory and the western Eger Graben*. GeoErlangen 2005, Exkursion 24–29.09.2005, pp. 46–50.
- Rudnick, R.L., Goldstein, S.L., 1990. The Pb isotopic compositions of lower crustal xenoliths and the evolution of lower crustal Pb. *Earth Planet. Sci. Lett.* 98, 192–207.
- Schaeffer, A.J., Lebedev, S., 2013. Global shear-speed structure of the upper mantle and transition zone. *Geophys. J. Int.* 194, 417–449.
- Schaeffer, A.J., Lebedev, S., 2015. Global heterogeneity of the lithosphere and underlying mantle: A seismological appraisal based on multimode surface-wave dispersion analysis, shear-velocity tomography, and tectonic regionalization. Invited Review. In: Khan, A., Deschamps, F. (Eds.), *"The Earth's Heterogeneous Mantle"*. Springer Geophysics, pp. 3–46 <http://dx.doi.org/10.1007/978-3-319-15627-9-1>.
- Schaeffer, A.J., Lebedev, S., Becker, T.W., 2016. Azimuthal seismic anisotropy in the Earth's upper mantle and the thickness of tectonic plates. *Geophys. J. Int.* 207, 901–933. <http://dx.doi.org/10.1093/gji/ggw309>.
- Scheck, M., Bayer, U., 1999. Evolution of the Northeast German Basin – inferences from a 3D structural model and subsidence analysis. *Tectonophysics* 313, 145–169.
- Scheck-Wenderoth, M., Lamarche, J., 2005. Crustal memory and basin evolution in the Central European Basin System—new insights from a 3D structural model. *Tectonophysics* 397, 143–165.
- Scheck-Wenderoth, M., Maystrenko, J., 2013. Deep control on shallow heat in sedimentary basins. *Energy Procedia* 40, 266–275.
- Scheck-Wenderoth, M., Krzywiec, P., Zühlke, R., Maystrenko, Y., Froitzheim, N., 2008. Permian to Cretaceous Tectonics. In: McCann, T. (Ed.), *The Geology of Central Europe Mesozoic and Cenozoic Vol. 2*. Geological Society of London, London, pp. 999–1030.
- Schmid, S.M., Kissling, E., 2000. The arc of the western Alps in the light of geophysical data on deep crustal structure. *Tectonics* 19, 62–85.
- Schmid, S.M., Pfiffner, O.A., Froitzheim, N., Schönborn, G., Kissling, E., 1996. Geophysical-geological transect and tectonic evolution of the Swiss-Italian Alps. *Tectonics* 15, 1036–1064.
- Schmincke, H.-U., 2007. The quaternary volcanic fields of the East and West Eifel (Germany). In: Ritter, R., Christensen, U. (Eds.), *Mantle Plumes A Multidisciplinary Approach*. Springer-Verlag, Berlin Heidelberg, pp. 241–322.
- Schmitt, A.K., Marks, M.A.W., Nesbort, H.D., Markl, G., 2007. The onset and origin of differentiated Rhine Graben volcanism based on U–Pb ages and oxygen isotopic composition of zircon. *Eur. J. Mineral.* 19, 849–857.
- Schott, B., Schmeling, H., 1998. Delamination and detachment of a lithospheric root. *Tectonophysics* 296, 225–247.
- Schreiner, A., 2008. Hegau und westlicher Bodensee. *Sammlung Geologischer Führer* 62. Berlin-Stuttgart, Gebrüder Bornträger.
- Schubert, S., Jung, S., Pfänder, J.A., Hauff, F., Garbe-Schönberg, D., 2015. Petrogenesis of tertiary continental intra-plate lavas between Siebengebirge and Westerwald, Germany: constraints from trace element systematics and Nd, Sr and Pb isotopes. *J. Volcanol. Geotherm. Res.* 305, 84–99.
- Schweitzer, J., 1995. Blockage of regional seismic waves by the Teisseyre-Tornquist zone. *Geophys. J. Int.* 123, 260–276.
- Seiberlich, C.K.A., Ritter, J.R.R., Wawerzinek, B., 2013. Topography of the lithosphere–asthenosphere boundary below the Upper Rhine Graben Rift and the volcanic Eifel region, Central Europe. *Tectonophysics* 603, 222–236.
- Soomro, R., Weidle, C., Cristiano, L., Lebedev, S., Meier, T., 2016. Phase velocities of Rayleigh and Love waves in central and northern Europe from automated, broad-band, interstation measurements. *Geophys. J. Int.* 204 (1), 517–534. <http://dx.doi.org/10.1093/gji/ggv462>.
- Spakman, W., 1990. Images of the upper mantle of central Europe and the Mediterranean. *Terra Nova* 2, 542–553.
- Stein, C.A., Stein, S., 1992. A model for the global variation in oceanic depth and heat flow with lithospheric age. *Nature* 359 (6391), 123–129.
- Stein, C.A., Stein, S., 2015. Are large oceanic depth anomalies caused by thermal perturbations? In: Foulger, G.R., Lustrino, M., King, S.D. (Eds.), *The Interdisciplinary Earth: A Volume in Honor of Don L. Anderson: Geological Society of America Special Paper 514 and American Geophysical Union Special Publication*. 71. [http://dx.doi.org/10.1130/2015.2514\(12\)](http://dx.doi.org/10.1130/2015.2514(12)).
- Stosch, H.G., 1987. Constitution and evolution of subcontinental upper mantle and lower crust in areas of young volcanism: differences and similarities between Eifel (F.R. Germany) and Tariat Depression (central Mongolia) as evidenced by peridotite and granulite xenoliths. *Fortschr. Mineral.* 65, 49–86.
- Stosch, H.G., Lugmair, G.W., 1986. Trace elements and Sr and Nd isotope geochemistry of peridotite xenoliths from the Eifel (West Germany) and their bearing on the evolution of the subcontinental lithosphere. *Earth Planet. Sci. Lett.* 80, 281–298.
- Tanner, D.C., Behrmann, J.H., 1995. The Variscan tectonics of the Moldanubian gneisses, Oberpfälzer Wald: a compressional history. *N. Jb. Geol. Paläont. (Abh.)* 197, 331–355.
- Tesaro, M., Kaban, M.K., Cloetingh, S., 2008. EUCRUST-07: a new reference model for the European crust. *Geophys. Res. Lett.* 35, L05313. <http://dx.doi.org/10.1029/2007GL032244>.
- Thiemens, M., Sprung, P., 2015. Multi-isotopic evidence from West-Eifel xenoliths. (AGU Fall Meeting San Francisco) <https://agu.confex.com/agu/fm15/meetingapp.cgi/Paper/84689>.
- Thybo, H., Pharaoh, T., Guterch, A. (Eds.), 2002. *The Trans European suture Zone II*. *Tectonophysics* 360 (314 pp).
- Torsvik, T.H., Smethurst, M.A., Burke, K., Steinberger, B., 2008. Long term stability in deep mantle structure: evidence from the ~300 Ma Skagerrak-Centered Large Igneous Province (the SCIP). *Earth Planet. Sci. Lett.* 267, 444–452.
- Trampert, J., Woodhouse, J.H., 1995. Global phase velocity maps of Love and Rayleigh waves between 40 and 150 seconds. *Geophys. J. Int.* 122, 675–690.
- Ulrych, J., Dostal, J., Adamovic, J., Jelinek, E., Spacek, P., Hegner, E., Balogh, K., 2011. Recurrent Cenozoic volcanic activity in the Bohemian Massif (Czech Republic). *Lithos* 123, 133–144.
- Ulrych, J., Dostal, J., Hegner, E., Balogh, K., Ackerman, L., 2008. Late Cretaceous to Paleocene melilitic rocks of the Ohre/Eger Rift in northern Bohemia, Czech Republic: insights into the initial stages of continental rifting. *Lithos* 101, 141–161.
- Ulrych, J., Pivec, E., Lang, M., Balogh, K., Kropacek, V., 1999. Cenozoic intraplate-volcanic rock series of the Bohemian Massif: a review. *Geolines* 9, 123–129.
- Van Balen, R.T., van Bergen, F., Pagnier, H., Simmelink, H.J., van Wees, J.D., Verweij, J.M., 2000. Modelling the hydrocarbon generation and migration in the West Netherlands Basin, the Netherlands. *Geologie en Mijnbouw/Netherlands Journal of Geosciences* 79, 29–44.
- van Wees, J.-D., Stephenson, R.A., Ziegler, P.A., Bayer, U., McCann, T., Dadlez, R., Gaupp, R., Narkiewicz, M., Bitzer, F., Scheck, M., 2000. On the origin of the Southern Permian Basin, Central Europe. *Mar. Pet. Geol.* 17, 43–59.
- Vaněčková, M., Holub, F.V., Souček, J., Bowes, D.R., 1993. Geochemistry and Petrogenesis of the Tertiary alkaline volcanic Suite of the Laba Labe Tectonovolcanic Zone, Czech Republic. *Mineral. Petrol.* 48, 17–34.
- Villaseñor, A., Ritzwoller, M.H., Levshin, A.L., Barmin, M.P., Engdahl, E.R., Spakman, W., Trampert, J., 2001. Shear velocity structure of central Eurasia from inversion of surface wave velocities. *Phys. Earth Planet. Inter.* 123, 169–184.
- Wedepohl, K.H., 1985. Origin of the Tertiary basaltic volcanism in the northern Hessian Depression. *Contrib. Mineral. Petrol.* 89, 122–143.
- Wedepohl, K.H., Baumann, A., 1999. Central European Cenozoic plume volcanism with OIB characteristics and indications of a lower mantle source. *Contrib. Mineral. Petrol.* 136, 225–239.
- Weidle, C., Maupin, V., 2008. An upper-mantle S-wave velocity model for Northern Europe from Love and Rayleigh group velocities. *Geophys. J. Int.* 175, 1154–1168.
- Wilson, M., Downes, H., 1991. Tertiary-Quaternary extension related alkaline magmatism in Western and Central Europe. *J. Petrol.* 32, 811–849.
- Wilson, M., Rosenbaum, J.M., Dunworth, E.A., 1995. Melilitites: partial melts of the thermal boundary layer? *Contrib. Mineral. Petrol.* 119, 181–196.
- Wimmenauer, W., 1974. The alkaline province of central Europe and France. In: Sorensen, H. (Ed.), *The Alkaline Rocks*. Wiley, London, pp. 286–291.
- Wimmenauer, W., 2003. Erläuterungen zum Blatt Kaiserstuhl. *Geologische Karte von Baden-Württemberg 1:25.000*. Hrsg. Landesamt für Geologie, Rohstoffe und Bergbau Baden-Württemberg, Freiburg i.Br., 280 S.
- Witt, G., Seck, H.A., 1989. Origin of amphibole in recrystallized and porphyroclastic mantle xenoliths from the Rhinisch Massif: implications for the nature of mantle metasomatism. *Earth Planet. Sci. Lett.* 91, 327–340.
- Witt-Eickchen, G., 2007. Thermal and geochemical evolution of the shallow subcontinental lithospheric mantle beneath the Eifel: constraints from Mantle Xenoliths, a Review. In: Ritter, R., Christensen, U. (Eds.), *Mantle Plumes A Multidisciplinary Approach*. Springer-Verlag, Berlin Heidelberg, pp. 323–338.

- Witt-Eickschen, G., Kramm, U., 1998. Mantle upwelling and metasomatism beneath central Europe: geochemical and isotopic constraints from mantle xenoliths from the Rhön (Germany). *J. Petrol.* 38, 479–493.
- Witt-Eickschen, G., Kaminsky, W., Kramm, U., Harte, B., 1998. The nature of young vein metasomatism in the lithosphere of the West Eifel (Germany): geochemical and isotopic constraints from composite mantle xenoliths from the Meerfelder Maar. *J. Petrol.* 39, 155–185.
- Witt-Eickschen, G., Seck, H.A., Mezger, K., Eggins, S.M., Altherr, R., 2003. Lithospheric mantle evolution beneath the Eifel (Germany): constraints from Sr-Nd-Pb isotopes and trace element abundances in spinel peridotite and pyroxenite xenoliths. *J. Petrol.* 44, 1077–1095.
- Zhou, Y., Nolet, G., Dahlen, F.A., Laske, G., 2006. Global upper-mantle structure from finite-frequency surface-wave tomography. *J. Geophys. Res.* 111, B04304.
- Zhu, H., Tromp, J., 2013. Mapping tectonic deformation in the crust and upper mantle beneath Europe and the North Atlantic. *Science* 341, 871. <http://dx.doi.org/10.1126/science.1241335>.
- Ziegler, P.A., 1990. Geological Atlas of Western and Central Europe, Shell Internat. Petrol. Mij., Dist. Geol. Soc. Publ. House, Bath. 2nd ed. (239 pp. and 56 encl).
- Ziegler, P.A., 1994. Cenozoic rift system of Western and Central Europe: an overview. *Geol. Mijnb.* 71, 99–127.
- Ziegler, P.A., 2002. European Cenozoic rift system. *Tectonophysics* 208, 91–111.
- Ziegler, P.A., Dèzes, P., 2006. Crustal evolution of Western and Central Europe. *Geol. Soc. Lond. Mem.* 32, 43–56.
- Zielhuis, A., Nolet, G., 1994. Shear-wave velocity variations in the upper mantle beneath central Europe. *Geophys. J. Int.* 117, 695–715.